Published November 8, 2010

JEM

SUPPLEMENTAL MATERIAL

Ebihara et al., http://www.jem.org/cgi/content/full/jem.20091573/DC1

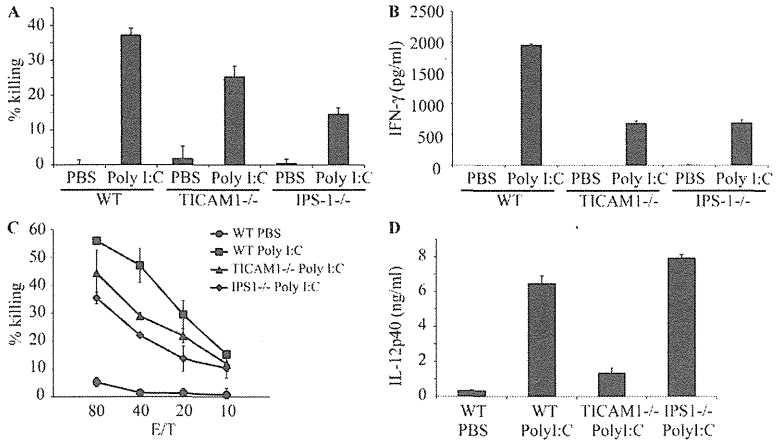

Figure S1. KO mice results suggest that both IPS-1 and TICAM-1 in BMDC participate in polyI:C-driven NK activation. (A and B) IPS-1 and TICAM-1 in BMDC participate in polyI:C-driven NK activation. 2.5 × 10^5 BMDCs prepared from WT, TICAM1$^{-/-}$, and IPS1$^{-/-}$ mice were incubated with 5 × 10^5 NK cells in the presence or absence (PBS) of 50 µg/ml polyI:C for 24 h. Then, the supernatants were harvested for IFN-γ ELISA (B). To determine NK cytotoxicity, ^{51}Cr-labeled B16D8 cells were added to the culture and, 4 h later, released ^{51}Cr was measured (A). One representative of three similar experiments is shown. (C) Both IPS-1 and TICAM-1 participate in in vivo polyI:C-induced NK activation. WT, IPS-1$^{-/-}$, and TICAM-1$^{-/-}$ mice were i.p. injected with 250 µg polyI:C. After 24 h, NK cells were harvested by DX5-MACS beads from spleen and used as effector cells in a cytotoxic assay with ^{51}Cr-labeled B16D8 targets. Cytotoxic activity of NK cells was measured under the indicated E/T ratios 4 h after the E/T mixing. One representative of the three similar experiments is shown. (D) Increasing serum level of IL-12p40 is dependent on TICAM-1. 250 µg polyI:C was i.p. injected into a series of mice as in B. 8 h after injection of polyI:C, blood serum was collected to determine the levels of IL-12p40 by ELISA. Although it is not depicted, IL-12p70 was not detected in these samples by ELISA. Data in A–D represent mean ± SD.

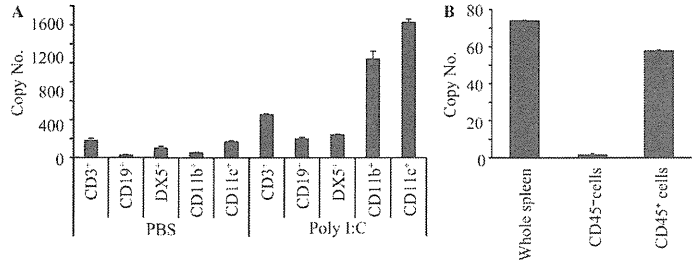

Figure S2. In vivo polyI:C response of INAM in LN cells. (A) Up-regulation of INAM expression in LN cells by polyI:C injection. WT C57BL/6 mice were i.p. injected with 100 µg polyI:C or control buffer. After 24 h, inguinal, axillary, and mesenteric LN were harvested. Cell populations with indicated markers were separated by FACS sorting, and the INAM mRNA level of each population was determined by real-time PCR. (B) CD45$^+$ cells express INAM. Splenocytes were separated into CD45$^-$ and CD45$^+$ cells after the polyI:C injection as in A. The INAM mRNA levels of the two populations were determined by real-time PCR. Representative data from one of three experiments are shown. Data in A and B represent mean ± SD.

Published November 8, 2010

JEM

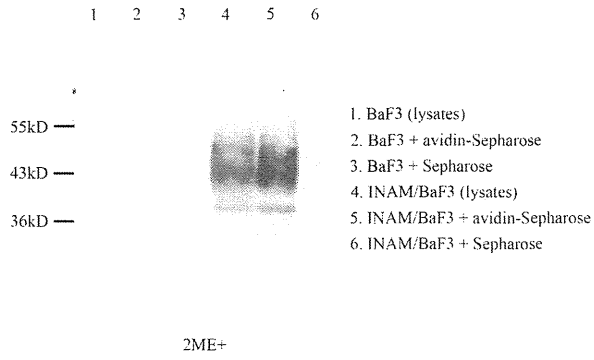

Figure S3. INAM is expressed on cell surface. Membrane proteins of Flag-tagged INAM-expressing BaF3 (INAM/BaF3) and control BaF3 were biotinylated and solubilized. Biotinylated proteins were immunoprecipitated by Avidin-Sepharose or control Sepharose. After electrophoresis on SDS-PAGE, INAM was detected by anti-Flag M2 mAb.

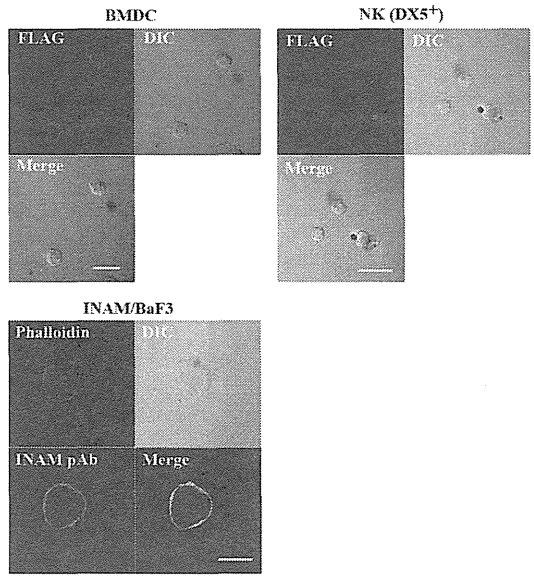

Figure S4. Confocal analysis of surface-expressed INAM. WT BMDC (left) or NK cells (right) were infected with INAM-expressing vector and stained with anti-FLAG mAb (Alexa Fluor 568). Stable Ba/F3 transfectants expressing INAM (bottom) were permeabilized and stained with phalloidin and anti-INAM pAb, followed by Alexa Fluor 488–conjugated secondary antibody. Cells were analyzed on a confocal laser-scanning microscope (LSM 510 META). Bars, 20 μm.

Published November 8, 2010

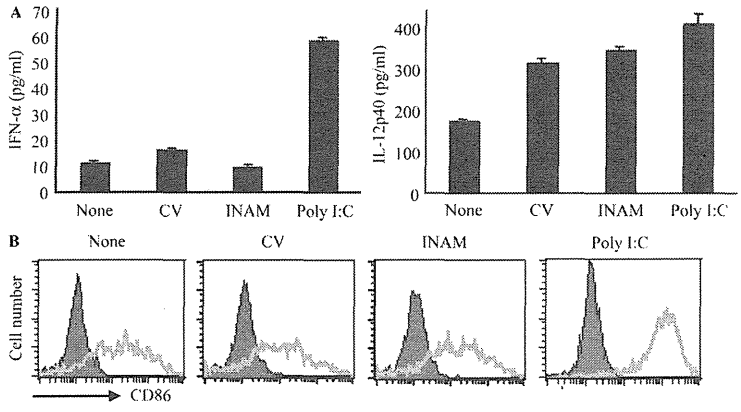

Figure S5. INAM-overexpressing BMDC did not induce cytokine responses and maturation. WT BMDCs were transfected with control lentivirus (CV) or INAM-expressing lentivirus (INAM-virus) and cultured for 24 h. (A) ELISA of IFN-α and IL-12p40 in the culture supernatants. Data shown are means ± SD of triplicate samples from one experiment representative of three. (B) Flow cytometry for CD86 in the transfected BMDC. PolyI:C stimulation (10 μg/ml) was used for positive control.

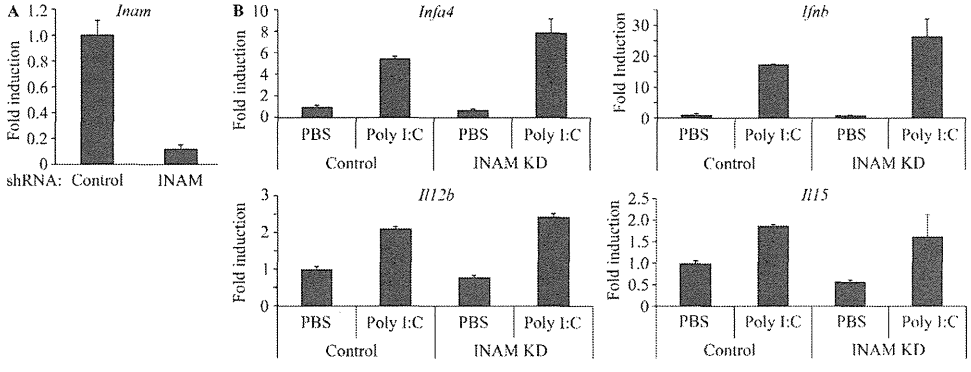

Figure S6. The effect of gene silencing of INAM on the polyI:C-mediated cytokine inducing profile in BMDC. (A) Gene silencing of INAM in BMDC. 5 × 10^5 WT BMDCs were infected with INAM shRNA-generating lentivirus or control lentivirus. After 36 h, the levels of INAM mRNA expression were assessed by real time PCR. Data show one of three similar experiments. (B) Effect of BMDC INAM on cytokine expression. INAM in 5 × 10^5 WT BM-DCs was silenced as in A. Then, control or INAM-silenced BMDC were stimulated with 10 μg/ml polyI:C for 8 h. RNA was harvested from BMDC with RNeasy and the levels of indicated mRNA were determined by real-time PCR. Data show one of two similar experimental results. Data in A and B represent mean ± SD.

Published November 8, 2010

JEM

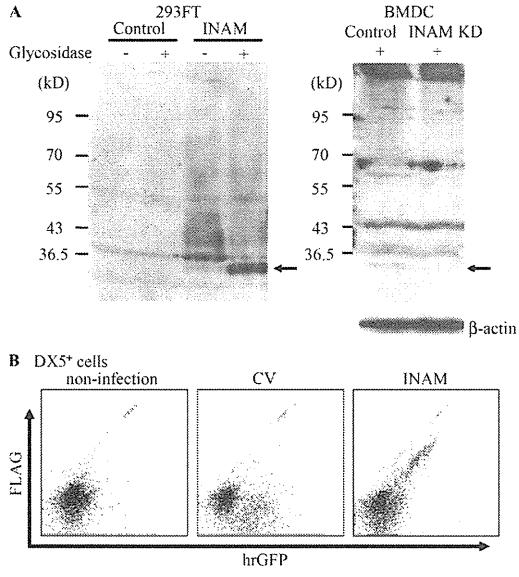

Figure S7. Detection of the INAM protein in DCs and NK cells. (A) Detection of the endogenous INAM protein in BMDC. 5 × 10^6 BMDCs were transduced with INAM-shRNA or control shRNA-expressing lentivirus. 48 h later, these cells were lysed and treated with *N*-glycosidase F for 2 h at 37°C. All cell lysates were subjected to SDS-PAGE and immunoblotted by rabbit anti-INAM pAb. The cell lysates from 293FT cells transfected with pEFBOS or pEFBOS/INAM were used as negative and positive control, respectively. Arrows indicate the band for INAM. Mr markers are shown to the left. One of three similar experiments is shown. (B) $DX5^+$ NK cells express GFP and FLAG, markers for INAM. 5 × 10^5 $DX5^+$ cells were transduced with control or INAM-expressing lentivirus for 48 h. Then, these cells were permeabilized and stained with rabbit anti-FLAG pAb and PE-anti rabbit IgG. Levels of FLAG and hrGFP, reflecting INAM expression, were measured by FACSCalibur. Experiments were performed more than six times with different conditions and representative data are shown.

Table S1. TICAM-1-inducible genes encoding putative membrane or GPI-anchored proteins

Official symbol	Other aliases	UniGene ID	Fold induction (poly I:C stimulation/nonstimulation)			
			WT	MyD88$^{-/-}$	TLR3$^{-/-}$	TICAM-1$^{-/-}$
Aplnr	APJ, Agtrl1, msr/apj	Mm.29368	2.074101377	0.79485698	0.24913528	0.296911294
Fam26f	INAM, A630077B13Rik	Mm.34479	15.57360865	8.048081457	0.939239821	1.221297574
Clec4e	Clecsf9, Mincle	Mm.248327	5.65851862	7.142025946	2.761541794	2.087684899
Ly6i	Ly-6M, AI789751	Mm.358339	5.679941154	26.36364231	0.734513568	1.09611157
Slamf8	Blame, SBBI42	Mm.179812	6.814581008	5.127202394	1.802731559	1.122849288
Tmem171	Gm905, MGC117733	Mm.28264	12.42279971	7.454421156	2.274145126	3.051240138
Pvrl4	1200017F15Rik, Prr4	Mm.263414	5.02297837	4.096701442	1.627391239	1.961829994
Vcam1	CD106	Mm.76649	4.742423155	4.572993249	0.948952117	0.554171652
Tnfsf10	APO-2L, TL2, Trail	Mm.1062	41.9745751	30.22262268	6.007858781	2.631939934

THE JOURNAL OF BIOLOGICAL CHEMISTRY VOL. 285, NO. 26, pp. 20128–20136, June 25, 2010

A Molecular Mechanism for Toll-IL-1 Receptor Domain-containing Adaptor Molecule-1-mediated IRF-3 Activation*[S]

Received for publication, December 24, 2009, and in revised form, March 25, 2010 Published, JBC Papers in Press, April 23, 2010, DOI 10.1074/jbc.M109.099101

Megumi Tatematsu[‡], Akihiro Ishii[‡1], Hiroyuki Oshiumi[‡], Masataka Horiuchi[§], Fuyuhiko Inagaki[§], Tsukasa Seya[‡], and Misako Matsumoto[‡2]

From the [‡]Department of Microbiology and Immunology, Hokkaido University Graduate School of Medicine, Kita 15, Nishi 7, Kita-ku, Sapporo 060-8638 and the [§]Department of Structural Biology, Graduate School of Pharmaceutical Science, Hokkaido University, N-21, W-11, Kita-ku, Sapporo 001-0021, Japan

The Toll-IL-1 receptor (TIR) domain-containing adaptor molecule-1 (TICAM-1, also called TRIF) is a signaling adaptor for TLR3 and TLR4 that activates the transcription factors IRF-3, NF-κB, and AP-1, leading to induction of type I interferon and cytokines. The N-terminal region of TICAM-1 participates in IRF-3 activation, although the C-terminal region is involved in NF-κB activation. However, the mechanism by which TICAM-1 is activated and transmits signals is largely unknown. In this study, we identified Leu^{194} as a critical amino acid for TICAM-1-mediated IRF-3 activation. When Leu^{194} was substituted with Ala, the mutant TICAM-1 failed to recruit the IRF-3 kinase TBK1, resulting in lack of IRF-3 phosphorylation, although TRAF3 and NAP1 appeared to be recruited. The N-terminal 176 amino acids of TICAM-1 (N-terminal domain (NTD)) form a protease-resistant structural domain. A TICAM-1 mutant lacking the N-terminal 180 amino acids showed greater interferon-β promoter activation than wild-type TICAM-1. Furthermore, immunoprecipitation and protein-protein interaction analysis revealed that the NTD interacted with the N terminus of TICAM-1-TIR. These results suggest that the NTD folds into the TIR domain structure to maintain the naive conformation of TICAM-1. Upon stimulation of TLR3/4, TICAM-1 oligomerizes through the TIR domain and the C-terminal region, which may break the intramolecular association and induce a conformational change that allows TBK1 access to TICAM-1.

The innate immune system senses microbial infection using Toll-like receptors and cytoplasmic pattern-recognition receptors, which rapidly induce an antimicrobial response (1). Recent studies have demonstrated that these receptors also recognize molecular patterns associated with tissue damage and induce cytokine and chemokine production, which may lead to a sterile inflammation and progression of autoimmune diseases (2). Downstream of each pattern-recognition receptor is a signaling adaptor protein that determines the nature of response by activating distinct transcription factors (3). The Toll-IL-1 receptor (TIR)[3] domain-containing adaptor molecule-1 (TICAM-1), which is also known as TIR domain-containing adaptor inducing IFN-β (TRIF), is a signaling adaptor for TLR3 and TLR4 that activates the transcription factors IRF-3, NF-κB, and AP-1, leading to induction of type I IFN and cytokines, as well as myeloid dendritic cell (mDC) maturation (4–7). The final response mediated by TICAM-1 depends on the cell type and the activating TLR3/4 ligand.

Poly(I-C) is a synthetic analog of viral double strand RNA that generates a unique maturation stage in mDCs via TLR3-TICAM-1-dependent gene expression, leading to activation of natural killer cells and cytotoxic T lymphocytes (8, 9). Monophosphoryl lipid A is a TLR4 ligand that activates mDCs to induce T cell immunity via TICAM-1 but not MyD88 (10), implying that TICAM-1 signaling is crucial for inducing effective cellular responses. In contrast, oxidized phospholipids generated by oxidative stress or virus infection activate cytokine production in lung macrophages through the TLR4-TICAM-1 pathway, and this is the key disease pathway in acute lung injury (11). Thus, specific stimuli have been discovered, but the mechanism by which TICAM-1 is activated by upstream pattern-recognition receptors and transmits downstream signals is largely unknown.

TICAM-1 is expressed at a low level in most tissues and cells and is diffusely localized in the cytoplasm of resting cells (4, 12). When endosomal TLR3 is activated by double strand RNA, TICAM-1 transiently colocalizes with TLR3 and then dissociates from the receptor and forms speckled structures that colocalize with downstream signaling molecules (12, 13). Upon

* This work was supported in part by grants-in-aid from the Ministry of Education, Science, and Culture, the Ministry of Health, Labor, and Welfare of Japan, The NorthTec Foundation, The Akiyama Life Science Foundation, Sapporo Biocluster "Bio-S" (Knowledge Cluster Initiative of Ministry of Education, Culture, Sports, Science and Technology), and the Program of Founding Research Centers for Emerging and Reemerging Infectious Diseases, Ministry of Education, Culture, Sports, Science and Technology.

[S] The on-line version of this article (available at http://www.jbc.org) contains supplemental Figs. 1 and 2.

[1] Present address: Dept. of Global Epidemiology, Hokkaido University Research Center for Zoonosis Control, Kita-20, Nishi-10, Kita-ku, Sapporo, 001-0020, Japan.

[2] To whom correspondence should be addressed. Tel.: 81-11-706-6056; Fax: 81-11-706-7866; E-mail: matumoto@pop.med.hokudai.ac.jp.

[3] The abbreviations used are: TIR, Toll-IL-1 receptor; DAPI, 4′,6-diamidine-2′-phenylindole dihydrochloride; mDC, myeloid dendritic cell; NTD, N-terminal domain (1–176 aa); RHIM, RIP homotypic interacting motif; TRAF, tumor necrosis factor receptor-associated factor; TRIF, TIR domain-containing adaptor-inducing IFN-β; aa, amino acid; PBS, phosphate-buffered saline; HA, hemagglutinin; IFN, interferon; Ab, antibody; mAb, monoclonal antibody; pAb, polyclonal antibody.

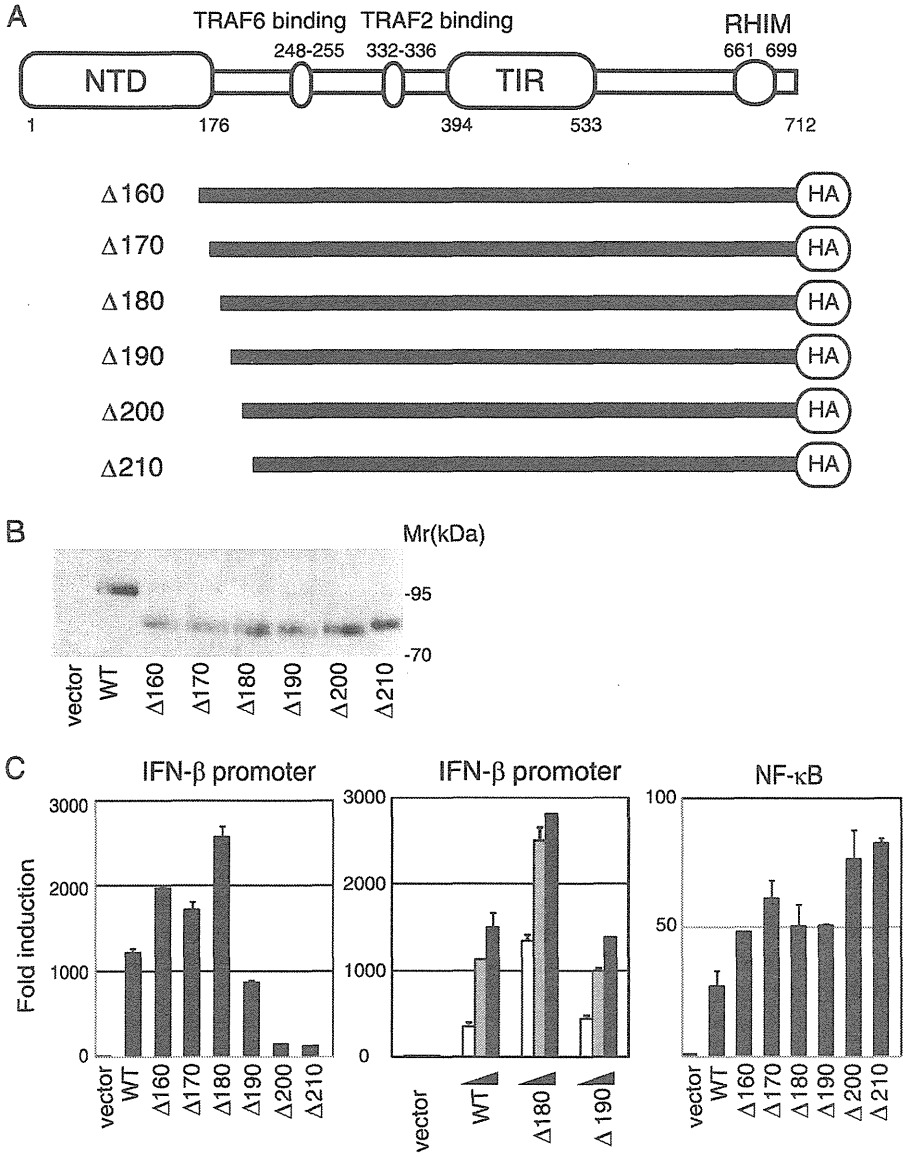

FIGURE 1. **TICAM-1 N-terminal region (191–200 aa) is essential for activation of the IFN-β promoter but not NF-κB.** *A*, schematic structure of human TICAM-1/TRIF and TICAM-1 mutants. *B*, protein expression of truncated TICAM-1 mutants in HEK293 cells. HEK293 cells in 24-well plates were transfected with the expression plasmids for HA-tagged wild-type TICAM-1 or TICAM-1 mutants (100 ng). Protein expression levels were determined by immunoblotting using anti-HA pAb. *C*, functional analysis of TICAM-1 mutants. HEK293 cells were transfected with empty vector or expression plasmid for wild-type (*WT*) TICAM-1 or each TICAM-1 mutant (Δ160–Δ210) (100 ng) together with the IFN-β promoter reporter (*left panel*) or NF-κB reporter plasmid (*right panel*), and phRL-TK. In some experiments, HEK293 cells were transfected with increasing amounts of expression vectors (10, 50, and 100 ng) (*center panel*). Luciferase activity was measured 24 h after transfection. Representative data from a minimum of four separate experiments, each performed in triplicate, are shown.

lipopolysaccharide stimulation, TICAM-1 is activated by endosomal TICAM-2 (also called TRIF-related adaptor molecule), which associates with the internalized TLR4 (14). Forced expression of TICAM-1 leads to homo-oligomerization through the TIR domain and the C terminus, forming a complex called the TICAM-1 signalosome (15). The TIR domain of TICAM-1 is essential for binding to the TIR domain of TLR3 and to TICAM-2. The N-terminal region of TICAM-1 participates in IRF-3 activation by recruiting the IRF-3-activating kinases, TANK-binding kinase 1 (TBK1) and inhibitor of nuclear factor κB kinase ϵ (also called IKKι) (16–18). The C-terminal region of TICAM-1 is involved in NF-κB activation and inducing apoptosis by binding the RIP1 at the receptor-interacting protein homotypic interacting motif (RHIM) domain (19, 20). The tumor necrosis factor receptor-associated factor (TRAF) 3 and NF-κB-activating kinase-associated protein 1 (NAP1) engage in TICAM-1-mediated activation of IRF-3 (21–23). Thus, although molecules involved in the TICAM-1-mediated signaling have been identified, the molecular mechanism for TICAM-1 activation remains unknown.

Recently, the N-terminal 176 amino acids (aa) of TICAM-1 (NTD) were found to form a protease-resistant structure of eight α-helices (24). In this study, we analyzed the structure-function relationship of TICAM-1 with a series of TICAM-1 mutants and identified the critical amino acid for TICAM-1-mediated IRF-3 activation. Moreover, we offer a structural model of the resting form of TICAM-1, in which NTD folds into the TIR domain structure, preventing homodimerization and access of downstream signaling molecules to TICAM-1.

EXPERIMENTAL PROCEDURES

Cell Culture and Reagents—HEK293 cells were maintained in Dulbecco's modified Eagle's medium low glucose (Invitrogen) supplemented with 10% heat-inactivated fetal calf serum (BIOSOURCE) and antibiotics. HEK293FT cells were maintained in Dulbecco's modified Eagle's medium high glucose supplemented with 0.1 mM nonessential amino acids, 10% heat-inactivated fetal calf serum, and antibiotics. HeLa cells were maintained in minimum essential media (Nissui, Tokyo, Japan) supplemented with 1% L-glutamine and 5% heat-inactivated fetal calf serum. Anti-FLAG M2 mAb, anti-HA pAb, 4′,6-diamidine-2′-phenylindole dihydrochloride (DAPI), and benzyloxycarbonyl-VAD-fluoromethyl ketone were from Sigma. Alexa Fluor®-conjugated secondary antibodies were from Invitrogen; anti-Myc mAb was from Neomarkers (Lab Vision

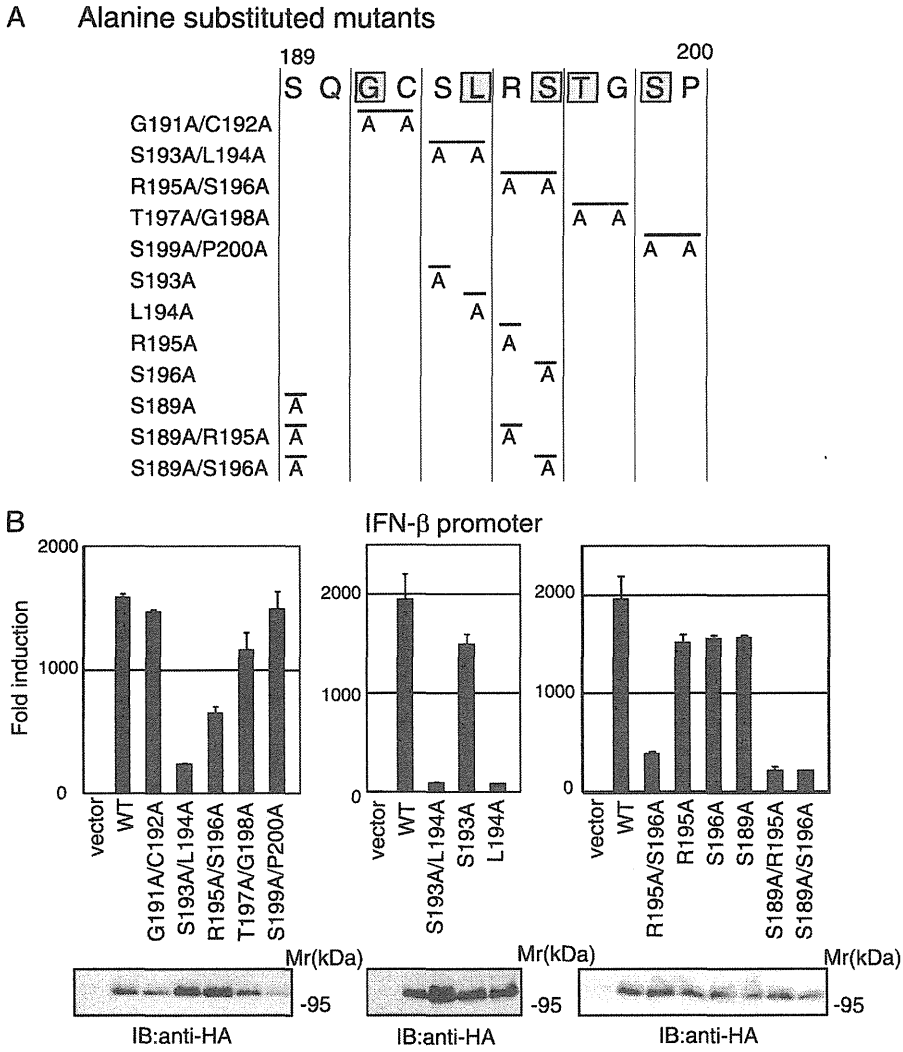

FIGURE 2. **Leu[194] is critical for TICAM-1-mediated IFN-β promoter activation.** *A*, amino acid sequence between Ser[189] and Pro[200] in TICAM-1. *Gray* indicates conserved residues between human and mouse. *B*, IFN-β promoter activation by alanine-substituted TICAM-1 mutants. HEK293 cells were transfected with empty vector or expression vectors for wild-type (*WT*) TICAM-1 or indicated alanine-substituted mutants, with the IFN-β promoter reporter and phRL-TK. Luciferase activity was measured 24 h after transfection. Representative data from a minimum of three separate experiments, each performed in triplicate, are shown. *Lower panels*, protein expression of alanine-substituted mutants in HEK293 cells. Cell lysates prepared in *A* were subjected to SDS-PAGE (7.5% gel) followed by immunoblotting (*IB*) with anti-HA pAb.

Corp., Fremont, CA); anti-HA mAb was from Covance (Emeryville, CA); anti-TBK1 pAb was from Abcam (Cambridge, MA); anti-human IRF3 rabbit IgG was from IBL (Gunma, Japan); horseradish peroxidase-conjugated secondary Abs were from BIOSOURCE; and poly(I-C) was from GE Healthcare.

Plasmids—Complementary DNAs for human TICAM-1, RIP1, TRAF2, TRAF3, and TRAF6 were cloned in our laboratory by reverse transcription-PCR and ligated into the cloning site of the expression vectors, pEF-BOS and p3×FLAG-CMV-14 (C-terminal 3×FLAG tag) (15). The pCDNA3.1/NAP1-Myc and pCDNA3.1/TBK1-FLAG expression vectors were kindly provided by Dr. M. Nakanishi (Nagoya City University, Nagoya, Japan). N-terminal deletion mutants of TICAM-1 (Δ160, Δ170, Δ180, Δ190, Δ200, and Δ210) were made by PCR with *Pfu* Turbo DNA polymerase (Stratagene, La Jolla, CA) using appropriate primers. pEF-BOS/TICAM-1-HA was used as a PCR template (33). Point mutations in TICAM-1 were generated by site-directed mutagenesis. Truncated TICAM-1 mutants TICAM-1-NTD (1–176 aa), TICAM-1-N (1–359 aa), TICAM-1-TIR (387–556 aa), and TICAM-1-C (534–712 aa) were generated by PCR using specific primers. An HA tag was inserted at the C terminus of each mutant.

Reporter Gene Assays—HEK293 cells (2×10^5 cells/well) cultured in 24-well plates were transfected with expression vectors for wild-type TICAM-1, TICAM-1 mutants, or empty vector, together with the reporter plasmid (100 ng/well) and an internal control vector, phRL-TK (Promega, Madison, WI) (5 ng/well) using FuGENE HD (Roche Diagnostics). The p-125 luciferase reporter contained the human IFN-β promoter (−125 to +19) and was provided by Dr. T. Taniguchi (University of Tokyo, Tokyo, Japan). A luciferase-linked NF-κB reporter gene and pAP-1-Luc reporter plasmid were from Stratagene. The total amount of DNA (500 ng/well) was kept constant by adding empty vector. After 24 h, cells were lysed in lysis buffer (Promega), and firefly and *Renilla* luciferase activities were determined using a Dual-Luciferase reporter assay kit (Promega). The firefly luciferase activity was normalized to the *Renilla* activity and expressed as the fold-stimulation relative to the activity of vector-transfected cells. All assays were performed in triplicate.

Confocal Microscopy—HeLa cells (1.0×10^5 cells/well) were plated onto micro cover glasses (Matsunami, Tokyo, Japan) in 12-well plates. The next day, cells were transfected with the indicated plasmids as above. For cells transfected with wild-type TICAM-1 or the L194A mutant, benzyloxycarbonyl-VAD-fluoromethyl ketone (20 μM) was added to the cells before transfection to inhibit apoptosis. 24 h after transfection, cells were fixed in acetone for 3 min and permeabilized with PBS containing 0.2% Triton X-100 for 10 min. Fixed cells were blocked in phosphate-buffered saline (PBS) containing 1% bovine serum albumin and labeled with the indicated primary Abs (3.0 μg/ml) for 60 min at room temperature. For staining endogenous TBK1, cells were fixed with 4% paraformaldehyde

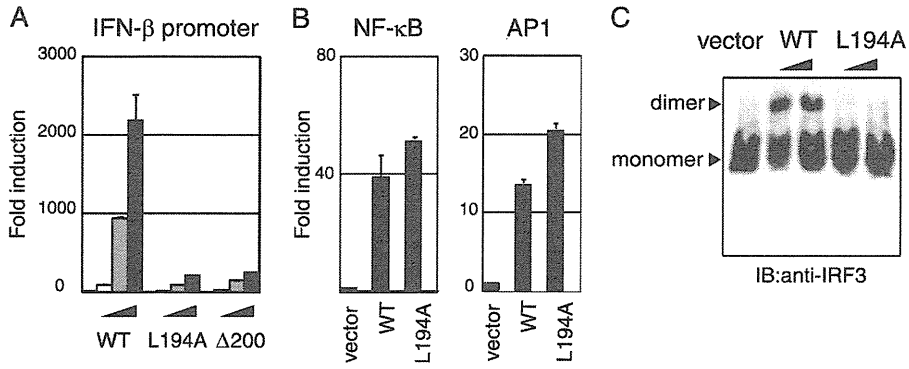

FIGURE 3. **Leu^{194} is critical for TICAM-1-mediated IRF-3 activation.** *A*, L194A mutant lost IFN-β promoter-activating ability. HEK293 cells were transfected with increasing amounts of wild-type (*WT*) TICAM-1 or L194A mutant expression vector (1, 10, and 100 ng) with an IFN-β reporter and phRL-TK. Luciferase activity was measured 24 h after transfection. Representative data from a minimum of three separate experiments are shown. *B*, L194A mutant activates NF-κB and AP-1. HEK293 cells were transfected with wild-type TICAM-1 or L194A mutant expression vector (100 ng) together with NF-κB (*left panel*) or AP-1 (*right panel*) reporters. *C*, L194A lost IRF-3 activating ability. HEK293 cells were transfected with empty vector, wild-type TICAM-1 vector, or L194A vector (100 and 400 ng). After 24 h, lysates were prepared and subjected to native PAGE. Monomeric and dimeric forms of IRF-3 (*arrowheads*) were detected by Western blot. *IB*, immunoblot.

for 10 min. Endogenous TBK1 was labeled with anti-TBK1 pAb (1:500). Alexa Fluor 488- or 594-conjugated secondary Abs (1:400) were used to visualize the primary Abs. Nuclei were stained with DAPI (2 μg/ml) in PBS for 10 min before mounting onto glass slides using PBS with 2.3% 1,4-diazabicyclo[2.2.2]octane and 50% glycerol. Cells were visualized at a 63× magnification with an LSM510 META microscope (Zeiss, Jena, Germany).

Immunoprecipitation and Immunoblotting—HEK293FT cells (5×10^5 cells/well) cultured in 6-well plates were transfected as above with the indicated plasmids. For wild-type TICAM-1 and the TICAM-1 mutants containing the RHIM domain, benzyloxycarbonyl-VAD-fluoromethyl ketone (20 μM) was added as described above. The total amount of DNA (2.0 μg/well) was kept constant with an empty vector. After 24 h, cells were lysed in lysis buffer (20 mM Tris-HCl, pH 7.5, containing 150 mM NaCl, 1% Nonidet P-40, 10 mM EDTA, 25 mM iodoacetamide, 2 mM phenylmethylsulfonyl fluoride, 5 mM Na_3VO_4 and a protease inhibitor mixture (Roche Diagnostics)). Lysates were pre-cleared with protein G-Sepharose (GE Healthcare) and incubated with 0.5 μg of anti-tag Abs or anti-TBK1 pAb (1:50). Immunocomplexes were recovered by incubation with protein G-Sepharose, washed five times with lysis buffer, and resuspended in denaturing buffer. Samples were analyzed by SDS-PAGE (7.5–12.5% gel) under reducing conditions followed by immunoblotting with anti-tag Abs. For immunoblotting, HEK293 cells cultured in 24-well plates were transfected with the indicated plasmids (100 ng). After 24 h, cells were lysed in lysis buffer. Lysates were clarified by centrifugation and subjected to SDS-PAGE (7.5% gel) followed by immunoblotting with anti-HA pAb.

Assay for IRF-3 Activation—HEK293 cells (2×10^5 cells/well) cultured in 24-well plates were transfected with wild-type TICAM-1 or TICAM-1 L194A mutant (0.1 and 0.4 μg) using Lipofectamine 2000 reagent (Invitrogen). The total amount of DNA (0.8 μg/well) was kept constant with an empty vector. After 24 h, cells were lysed in lysis buffer (50 mM Tris-HCl, pH 8.0, containing 150 mM NaCl, 1% Nonidet P-40, 100 ng/ml leupeptin, 1 mM phenylmethylsulfonyl fluoride, and 5 mM Na_3VO_4). Lysates were clarified by centrifugation (15,000 rpm, 10 min) and subjected to native-PAGE (7.5% gel) as described previously (34). Immunoblotting was performed using rabbit anti-human IRF-3 antibody and horseradish peroxidase-conjugated goat anti-rabbit IgG.

Protein-Protein Interaction Analysis—Protein-protein association in living cells was analyzed using the *CoralHue* Fluo-chase kit (MBL, Nagoya, Japan), which detects protein-protein interactions as fluorescent signals using the protein fragment complementation method. TICAM-1 NTD and TICAM-1-TIR cDNAs were subcloned into fusion protein expression plasmids according to the manufacturer's instructions. The *TICAM-1* NTD gene was fused to the 3′-end of the divided monomeric Kusabira-Green (*mKG*) gene N- or C-terminal fragment (mKGN-NTD and mKGC-NTD), and the *TICAM-1*-TIR gene was fused to the 5′- or 3′-end of the *mKG* gene N- or C-terminal fragment (TIR-mKGN, TIR-mKGC, mKGN-TIR, and mKGC-TIR). HEK293FT cells (5×10^5 cells/well) cultured in 6-well plates were transfected with the indicated combinations of plasmids as above. After 24 h, the conditioned media were replaced with Dulbecco's PBS, and fluorescent living cells were visualized with fluorescent microscopy (Olympus).

RESULTS

TICAM-1 N Terminus from Gly^{191} to Pro^{200} Is Essential for IFN-β Promoter Activation—The N terminus of TICAM-1 contains TRAF6- and TRAF2-binding sites (Fig. 1*A*). Limited trypsin digestion of TICAM-1 (1–556 aa) for 4 h generates the N-terminal fragment TICAM-1(1–176), and 20 h of digestion yields the fragment TICAM-1(1–156) (24). To examine the role of the TICAM-1 N-terminal domain, we made a series of truncated constructs (Δ160–Δ210) and assayed NF-κB and IRF-3 activation by reporter assay. The protein expression levels of these mutants were approximately equivalent to wild type (Fig. 1*B*). TICAM-1-mediated IFN-β promoter activation was enhanced by deletion of the N-terminal 160, 170, or 180 aa, whereas the TICAM-1-mutant lacking the N-terminal 190 aa (Δ190) showed less activity than wild-type TICAM-1 (Fig. 1*C*, *left* and *center panels*). Interestingly, a TICAM-1 mutant lacking the N-terminal 200 or 210 aa (Δ200, Δ210) showed dramatic loss of activity. NF-κB activation ability, however, was enhanced in all the mutants (Fig. 1*C*, *right panel*). These results indicated that the N-terminal amino acids between Gly^{191} and Pro^{200} are essential for TICAM-1-mediated IFN-β promoter activation but not for NF-κB activation.

Leu^{194} *Is Critical for TICAM-1-mediated IFN-β Promoter Activation*—To identify residues crucial for TICAM-1-mediated IFN-β promoter activation, we performed alanine scanning of the region between Gly^{191} and Pro^{200} (Fig. 2*A*). Alanine-substituted mutants were expressed in HEK293 cells with an IFN-β reporter gene, and IFN-β promoter activation was assessed after 24 h. Western blot showed that the mutated proteins were expressed at levels similar to wild-type TICAM-1 in HEK293 cells (Fig. 2*B*, *lower panels*). Similar to the Δ200 mutant, the S193A/L194A mutant showed no activity, and the R195A/S196A mutant had partially diminished activity (Fig. 2*B*, *left panel*). Other mutations had no effect on the ability to activate the IFN-β promoter. Because substitution of Ser^{193} and Ser^{196} caused dysfunctional mutants, we made the additional single aa-substituted mutants S193A, L194A, R195A, S196A, and S189A and the combinations S189A/R195A and S189A/S196A, and we examined the role of these residues in TICAM-1 signaling (Fig. 2*A*). Remarkably, the substitution of Leu^{194} with Ala completely abolished IFN-β promoter-activation ability, whereas other single aa substitutions only slightly decreased activity. Both S189A/R195A and S189A/S196A mutants showed severely reduced activity (Fig. 2*B*, *center* and *right panels*). These results suggested that Leu^{194} is a critical amino acid for TICAM-1-mediated IFN-β promoter activation and that Ser^{189}, Arg^{195}, and Ser^{196} near Leu^{194} are associated with this promoter activation.

Leu^{194} *Is Indispensable for TICAM-1-mediated IRF-3 Activation*—The L194A mutant did not activate the IFN-β promoter, even though its expression was comparable with wild-type TICAM-1 (Fig. 3*A*). The promoter of the human IFN-β gene possesses binding sites for IRF-3, NF-κB, and AP-1 (25), so we examined which activation pathways were affected by mutation of Leu^{194}. As shown in Fig. 3*B*, substitution of Leu^{194} with Ala did not affect NF-κB- and AP-1-activation. In contrast, the ability to activate IRF-3 was abolished in the L194A mutant. Phosphorylation and dimer formation of IRF-3 were induced by the forced expression of wild-type TICAM-1 but not the L194A mutant in HEK293 cells (Fig. 3*C*), which suggested that

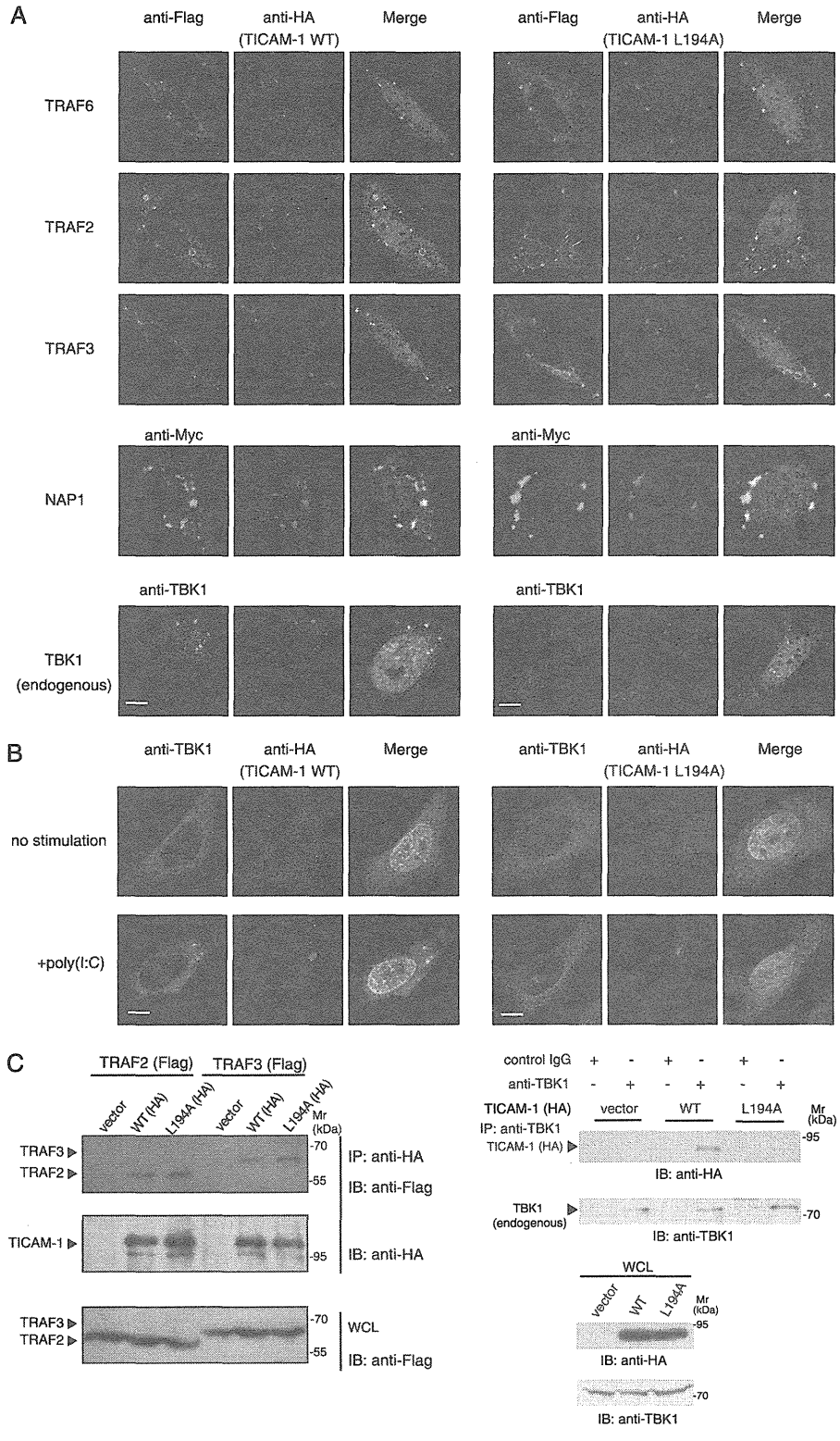

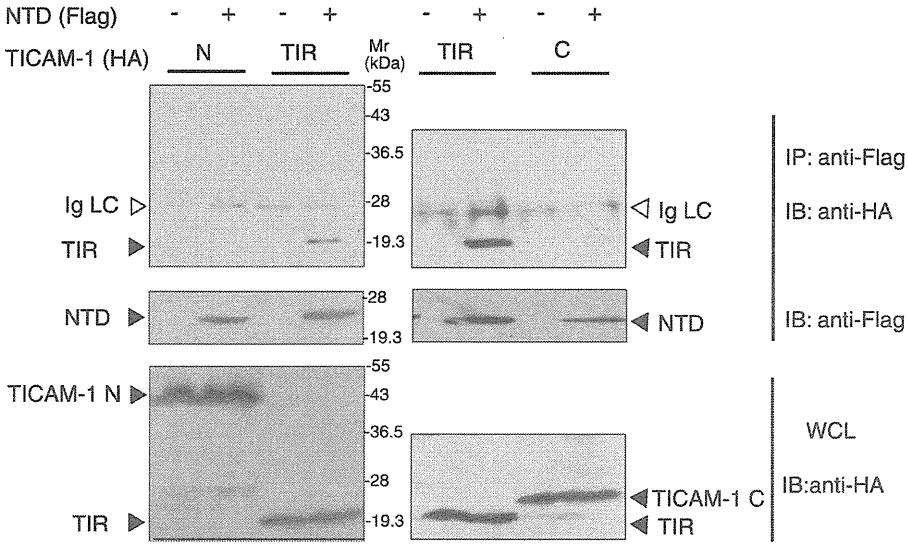

FIGURE 5. **NTD physically associates with TICAM-1-TIR.** HEK293FT cells were transfected with FLAG-tagged NTD and HA-tagged TICAM-1-N (1–359 aa), TIR domain (387–566 aa), or TICAM-1-C (567–712 aa). After 24 h, cells were lysed, and NTD was immunoprecipitated (*IP*) using an anti-FLAG mAb. The immunoprecipitants were resolved on SDS-PAGE (12.5% gel) under reducing conditions followed by immunoblotting (*IB*) with anti-HA pAb or anti-FLAG mAb. Whole cell lysates (*WCL*) were subjected to immunoblotting with anti-HA pAb to detect protein expression. *Open arrowheads* indicate immunoglobulin light chain (*Ig LC*). Molecular weight markers are on the *right*.

Leu^{194} is indispensable for TICAM-1-mediated IRF-3 activation.

Leu^{194} Is a Critical Amino Acid for Recruitment of TBK1 to TICAM-1—TRAF3 is an essential signaling molecule for TICAM-1-mediated IRF-3 activation (22, 23), and TRAF6 and TRAF2 directly bind to the N terminus of TICAM-1 through distinct binding sites (26). We analyzed the recruitment of TRAF family members to wild-type TICAM-1 or the L194A mutant by immunofluorescence staining and confocal microscopy. When HeLa cells were cotransfected with expression plasmids for HA-tagged wild-type or mutated TICAM-1, and FLAG-tagged TRAF6, TRAF2, or TRAF3, TRAF proteins colocalized with the L194A mutant as with the wild type (Fig. 4*A*). These results were confirmed by immunoprecipitation (Fig. 4*C*, *left panel*). We next examined whether Leu^{194} is required for recruitment of NAP1 and TBK1. NAP1, which is essential for TICAM-1-mediated IRF-3 activation and functions downstream of TRAF3, colocalized with both wild-type and the L194A mutant (Fig. 4*A*). However, the IRF-3 kinase TBK1 did not colocalize with the L194A mutant.

The lack of association between the L194A mutant and endogenous TBK1 was also observed in TLR3-mediated activation. Wild-type and the L194A mutant diffusely localized in cytoplasm when expressed at a low level (Fig. 4*B*). After poly(I-C) stimulation, wild-type TICAM-1 formed a speckle-like signalosome where endogenous TBK1 colocalized (Fig. 4*B*, *left panels*). In contrast, the L194A mutant did not recruit TBK1 to its signalosome (Fig. 4*B*, *right panels*). We analyzed physical association of TBK1 with wild-type or the L194A mutant by immunoprecipitation. Overexpressed HA-tagged wild-type TICAM-1 was coimmunoprecipitated with endogenous TBK1, although the L194A mutant was not (Fig. 4*C*, *right panels*). These results indicate that Leu^{194} is a key amino acid for recruitment of TBK1.

TICAM-1 NTD Interacts with the TICAM-1-TIR Domain—We previously showed that recruitment of NAP1 and TBK1 to TICAM-1 requires homo-oligomerization through the TIR domain and the C terminus and RIP1 binding to the RHIM domain (15). Upon TLR3/4 ligand stimulation, homo-oligomerization is triggered by binding to dimerized TLR3 or TICAM-2, and overexpression of TICAM-1 induces homo-oligomerization (15). How TICAM-1 molecules are prevented from auto-activation in the resting state remains unresolved. TICAM-1 contains two structural domains, the NTD and the TIR domain, and Leu^{194} and the TRAF2/6-binding sites are between these domains. We hypothesized that these interacting sites are covered by the NTD to prevent downstream signaling molecules from accessing TICAM-1.

To test this hypothesis, we investigated the physical association of the NTD with truncated TICAM-1 fragments. FLAG-tagged NTD was coexpressed with HA-tagged TICAM-1-N, TICAM-1-TIR, or TICAM-1-C in HEK293FT cells, and coimmunoprecipitation was performed using anti-tag Abs. Notably, NTD coimmunoprecipitated with TICAM-1-TIR but

FIGURE 4. **Leu^{194} is indispensable for recruitment of TBK1 to TICAM-1.** *A*, confocal images show HeLa cells coexpressing HA-tagged wild-type (*WT*) TICAM-1 (*left panels*) or L194A mutant (*right panels*) and FLAG-tagged TRAF6, TRAF2, and TRAF3 or Myc-tagged NAP1. HeLa cells, transfected with the expression plasmids for HA-tagged wild-type TICAM-1 or L194A mutant (50 ng) and the indicated FLAG- or Myc-tagged signaling molecules (300 ng), were stained with anti-FLAG or anti-Myc mAb and anti-HA pAb, followed by Alexa Fluor 488-labeled goat anti-mouse Ab and Alexa Fluor 568-labeled goat anti-rabbit Ab. Colocalization of TICAM-1 with endogenous TBK1 was detected using anti-TBK1 pAb and Alexa Fluor 488-labeled goat anti-rabbit Ab. *Red*, wild-type and L194A mutant; *green*, TRAF6, TRAF2, TRAF3, NAP1, and TBK1; *blue*, DAPI-stained nuclei. *Bar*, 10 μm. *B*, recruitment of endogenous TBK1 to TICAM-1 by poly(I-C) stimulation. HeLa cells were transfected with the expression vector for HA-tagged wild-type TICAM-1 or L194A mutant (0.1 ng). Twenty four hours after transfection, cells were stimulated with buffer alone or 10 μg/ml poly(I-C) for 30 min. Fixed cells were labeled with anti-HA mAb and anti-TBK1 pAb, followed by Alexa Fluor 568-labeled goat anti-mouse IgG and Alexa Fluor 488-labeled goat anti-rabbit IgG. *C*, endogenous TBK1 physically associates with wild-type TICAM-1 but not the L194A mutant. *Left panels*, HEK293FT cells were transfected with empty vector or expression vectors for HA-tagged wild-type (*WT*) TICAM-1 or L194A mutant together with FLAG-tagged TRAF2, TRAF3. After 24 h, cells were lysed, and TICAM-1 was immunoprecipitated using an anti-HA pAb. *Right panels*, cells were transfected with empty vector or expression vector for HA-tagged wild-type TICAM-1 or L194A mutant. After 24 h, cells were lysed, and endogenous TBK1 was immunoprecipitated (*IP*) using an anti-TBK1 pAb. Rabbit IgG was used as a control Ab. The immunoprecipitants were resolved on SDS-PAGE (7.5% gel) under reducing conditions followed by immunoblotting (*IB*) with anti-tag mAb or anti-TBK1 pAb. Whole cell lysates (*WCL*) were subjected to immunoblotting with anti-FLAG mAb, anti-HA pAb, or anti-TBK1 pAb to detect protein expression (*IB*). Molecular weight markers are on the *right*.

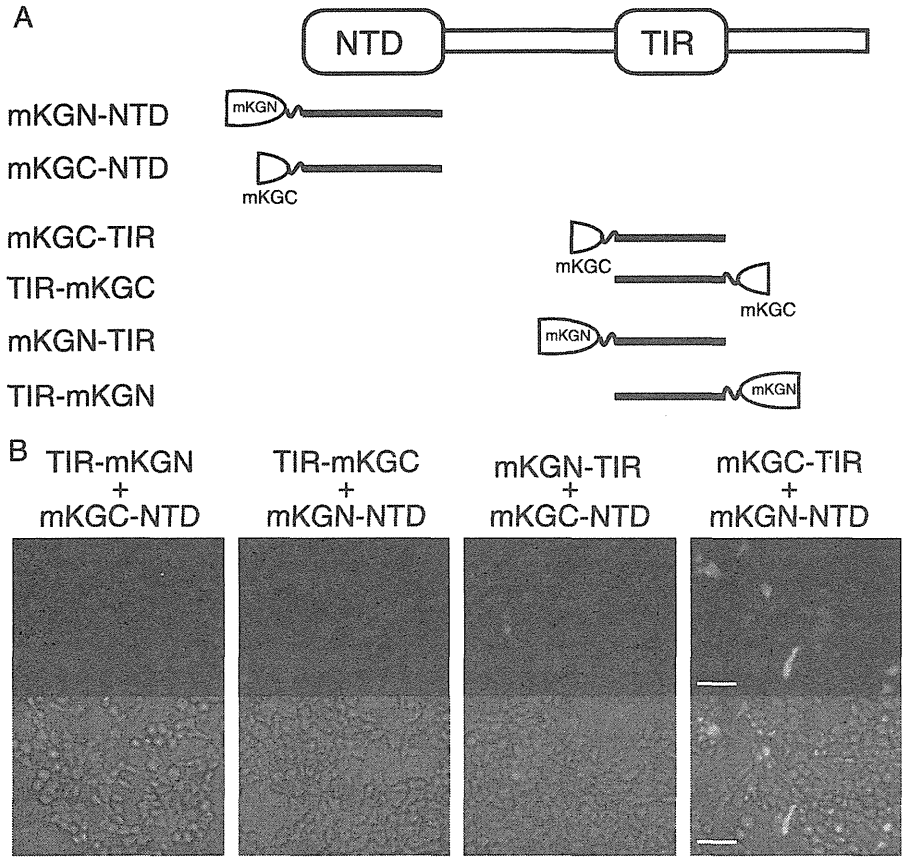

FIGURE 6. **NTD interacts with the N-terminal TICAM-1-TIR.** *A*, NTD or TICAM-1-TIR was fused to mKG fragments. *B*, fluorescence images show HEK293FT cells coexpressing NTD and TICAM-1-TIR, fused to mKG fragments at the N or C terminus. HEK293FT cells were transfected with the indicated combinations of expression plasmids for truncated TICAM-1 mutants fused to mKG fragments (each 500 ng). Twenty four hours after transfection, conditioned media were replaced with Dulbecco's PBS. Cells were visualized by fluorescence microscopy. Signal was detected in cells coexpressing mKGC-TIR and mKGN-NTD, and faint fluorescence was observed in cells coexpressing mKGN-TIR and mKGC-NTD. *Bar*, 100 μm.

not with TICAM-1-N or TICAM-1-C (Fig. 5), suggesting an intramolecular association between the NTD and the TIR domain. To further assess direct interaction between the NTD and the TIR domain, protein-protein interaction analysis was performed using a protein fragment complementation method. We made six constructs fusing the N- or C-terminal fragment of the monomeric Kusabira-Green protein to the N terminus of the NTD (mKGN-NTD, mKGC-NTD), the N terminus of the TIR domain (mKGN-TIR, mKGC-TIR), or the C terminus of the TIR domain (TIR-mKGN, TIR-mKGC) (Fig. 6*A*). Fluorescence was detected when expressed fused proteins interacted, restoring the mKG protein from the mKG fragments. HEK293FT cells were transfected with combinations of expression plasmids, and 24 h after transfection, strong fluorescent signals were detected in cells coexpressing mKGC-TIR and mKGN-NTD, and faint signals were detected in the cells coexpressing mKGN-TIR and mKGC-NTD (Fig. 6*B*). In contrast, cells coexpressing TIR-mKGN or TIR-mKGC and mKG-NTD did not fluoresce (Fig. 6*B*). These results strongly suggested that the NTD interacts with the N-terminal TICAM-1-TIR domain.

A TICAM-1 mutant lacking the NTD (Δ180) had high potential to activate the IFN-β promoter compared with wild-type TICAM-1 (Fig. 1*C*). This augmented activity of Δ180 mutant was more clearly shown when wild-type or Δ180 mutant was expressed at a low level (Fig. 7*A*). In HEK293 cells transfected with 0.1 ng of wild-type- or the L194A-expressing plasmid, wild-type TICAM-1 was inactive, whereas Δ180 mutant exerted the ability to activate the IFN-β promoter, although their protein expression levels were almost equivalent (Fig. 7*B*). Under these conditions, wild-type TICAM-1 diffusely localized in cytoplasm (Fig. 7*C*). In contrast, Δ180 mutant formed a speckle-like signalosome in unstimulated cells as seen in poly(I-C)-stimulated wild-type TICAM-1 (Fig. 7*C*), suggesting that deletion of the NTD facilitates the homo-oligomerization of Δ180 mutant through the TIR domain.

DISCUSSION

Activation of the transcription factor IRF-3 is a key downstream event in the signaling cascade of TICAM-1, resulting in induction of antiviral genes, including IFN-β. Direct binding of TICAM-1 to the IRF-3 activating kinase TBK1 is necessary for IRF-3 phosphorylation. Here, we identified Leu^{194} as essential in TICAM-1 for recruiting TBK1. Although Leu^{194} was critical for TBK1 binding, Ser^{189}, Arg^{195}, and Ser^{196} may stabilize the interaction.

TICAM-1 has two structural domains, the NTD and the TIR domain. Results from trypsin digestion of the TICAM-1 (1–566 aa) suggest the region between the NTD and the TIR domain forms a loose structure that might recruit downstream signaling molecules (24). Because the crucial amino acids for TRAF2, TRAF6, and TBK1 binding reside in this region, naive TICAM-1 may have a closed conformation that covers these sites. Indeed, using the protein-protein association analysis, we clearly showed that the NTD interacted with the N-terminal TIR domain. These observations suggest that the NTD folds into the TIR domain, preventing downstream signaling molecules from accessing their binding sites. Upon stimulation of TLR3/4, or TICAM-1 overexpression, TICAM-1 oligomerizes through the TIR domain and the C-terminal region (15). This may break the intramolecular association and induce a conformational change that allows downstream signaling molecules to their binding sites.

Deletion of the NTD augmented the TICAM-1 activity (Fig. 7). The association sites of TRAF2/6 and TBK1 are likely to be available in the Δ180 mutant. This would facilitate recruitment

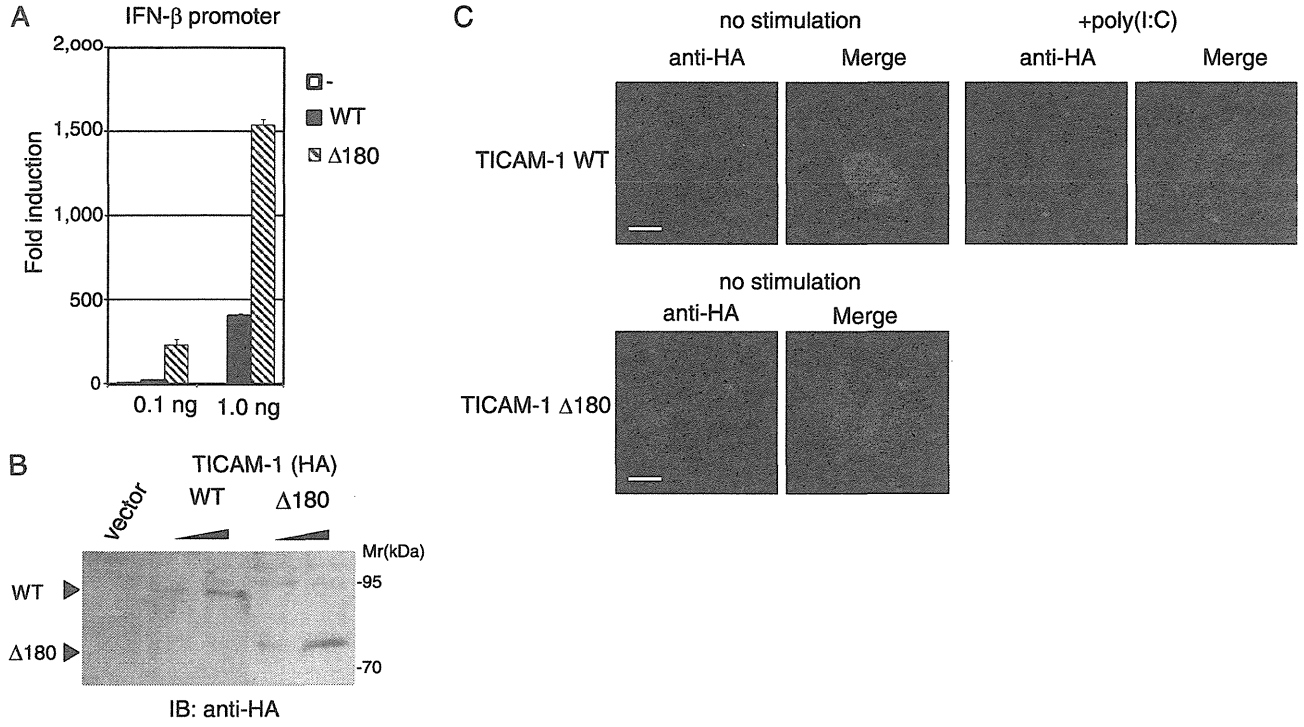

FIGURE 7. **Δ180 mutant had high potential to activate the IFN-β promoter compared with wild-type TICAM-1.** *A*, IFN-β promoter activation by the Δ180 mutant. HEK293 cells were transfected with empty vector or expression plasmid for wild-type (*WT*) TICAM-1 or Δ180 mutant (0.1 and 1.0 ng) together with the IFN-β promoter reporter. Luciferase activity was measured 24 h after transfection. Representative data from a minimum of four separate experiments, each performed in triplicate, are shown. *B*, protein expression of wild-type and the Δ180 mutant in HEK293 cell lysates. *IB*, immunoblot. *C*, confocal images of HeLa cells expressing a low level of HA-tagged wild-type TICAM-1 (*upper panels*) or Δ180 mutant (*lower panels*). Cells were transfected with the expression plasmid for wild-type TICAM-1 or Δ180 mutant (0.1 ng). After 24 h, cells were stimulated with buffer alone or 10 μg/ml poly(I-C) for 30 min, and fixed cells were labeled with anti-HA pAb and Alexa Fluor 568-labeled secondary Ab. The Δ180 mutant formed a speckle-like signalosome in unstimulated cells. *Red*, wild-type and Δ180 mutant; *blue*, DAPI-stained nuclei. *Bar*, 10 μm.

of the IRF-3 kinase complex. The Δ190 mutant showed reduced IFN-β promoter activation compared with the Δ180 mutant, probably because the absence of Ser^{189} stabilized TBK1 binding to TICAM-1 (Fig. 1*C*). Thus, the NTD may act as a repression domain within TICAM-1. Remarkably, exogenous NTD did not affect activation of IRF-3 or NF-κB by wild-type TICAM-1, the Δ180 mutant, or by TLR3-TICAM-1 activated with poly(I-C) (supplemental Fig. 1). We propose that exogenous NTD failed to interact with naive TICAM-1 because the TIR domain was occupied intramolecularly with NTD. Once TICAM-1 was recruited to TLR3, and oligomerized, the TRAF2/6 and TBK1 association sites appeared and signaling occurred quickly. When expressed with mutant Δ180, exogenous NTD interacted with the TIR domain of Δ180, whose binding site is distant from the TBK1 association sites, and did not affect TBK1 recruitment.

RIP1 binding to the C-terminal RHIM domain is necessary for TICAM-1 to mediate NF-κB activation (18), and the L194A mutant recruited RIP1 and activated NF-κB (Fig. 3*B* and supplemental Fig. 2). How NF-κB activation is controlled when TICAM-1 is in the resting form is unknown, but we surmise that the RHIM domain is unexposed in the resting state and that homodimerization opens the RHIM domain for RIP1 binding. Pro^{434} in the BB loop of the TICAM-1-TIR domain is critical for TICAM-1 homodimerization, but the C-terminal homodimerization determinant remains unidentified (15). Further analysis is required to elucidate the mechanism of TICAM-1 activation.

TICAM-1 acts as a platform that accumulates signaling molecules to the TICAM-1 signalosome and triggers diversified cellular responses. TICAM-1-dependent gene expression directs mDCs to activate natural killer cells and cytotoxic T lymphocytes, which are both the most effective for antiviral response, and are an anti-cancer immune response (8, 9). Indeed, TLR3/4 ligands are strong candidates for adjuvant anti-cancer and infectious disease immunotherapy (10, 27–29). Interestingly, the RIG-I-like receptor-mediated signaling pathway shares most of its downstream signaling molecules with the TICAM-1 pathway, but it plays a distinct role in antivirus immunity by producing type I IFNs (30). Although TICAM-1-mediated signaling is initiated from the endosome, RIG-I-like receptor-mediated signaling occurs at the mitochondrial outer membrane (31). Hence, compartmentalization of signal platforms might be significant for activating distinct transcription factors, resulting in different cellular responses.

In certain RNA viral infections, TLR3-TICAM-1-dependent inflammatory cytokine and chemokine production affects virally induced pathology and host survival (32). In addition, biased activation of the TLR4-TICAM-1 pathway in lung macrophages by oxidized phospholipids triggers acute lung injury through cytokine production (11). Therefore, control of TICAM-1 activation is a novel therapeutic target for acute lung

injury. The development of an inhibitory molecule that blocks homo-oligomerization of TICAM-1 might be a straightforward approach for controlling excessive activation of TICAM-1 after viral infection.

Acknowledgments—We are grateful to M. Sasai, K. Funami, A. Watanabe, H. Takaki, H. Shime, and T. Ebihara for invaluable discussions. Thanks are also due to T. Taniguchi (University of Tokyo) and M. Nakanishi (Nagoya City University, Nagoya, Japan) for providing the plasmids and to K. Arimoto (Kyoto University, Kyoto, Japan) and K. Shimotohno (Chiba Institute of Technology, Chiba, Japan) for providing reagents.

REFERENCES

1. Akira, S., Uematsu, S., and Takeuchi, O. (2006) *Cell* **124,** 783–801
2. Baccala, R., Hoebe, K., Kono, D. H., Beutler, B., and Theofilopoulos, A. N. (2007) *Nat. Med.* **13,** 543–551
3. O'Neill, L. A., and Bowie, A. G. (2007) *Nat. Rev. Immunol.* **7,** 353–364
4. Oshiumi, H., Matsumoto, M., Funami, K., Akazawa, T., and Seya, T. (2003) *Nat. Immunol.* **4,** 161–167
5. Yamamoto, M., Sato, S., Hemmi, H., Hoshino, K., Kaisho, T., Sanjo, H., Takeuchi, O., Sugiyama, M., Okabe, M., Takeda, K., and Akira, S. (2003) *Science* **301,** 640–643
6. Fitzgerald, K. A., Rowe, D. C., Barnes, B. J., Caffrey, D. R., Visintin, A., Latz, E., Monks, B., Pitha, P. M., and Golenbock, D. T. (2003) *J. Exp. Med.* **198,** 1043–1055
7. Oshiumi, H., Sasai, M., Shida, K., Fujita, T., Matsumoto, M., and Seya, T. (2003) *J. Biol. Chem.* **278,** 49751–49762
8. Schulz, O., Diebold, S. S., Chen, M., Näslund, T. I., Nolte, M. A., Alexopoulou, L., Azuma, Y. T., Flavell, R. A., Liljeström, P., Reis, e., and Sousa, C. R. (2005) *Nature* **433,** 887–892
9. Akazawa, T., Ebihara, T., Okuno, M., Okuda, Y., Shingai, M., Tsujimura, K., Takahashi, T., Ikawa, M., Okabe, M., Inoue, N., Okamoto-Tanaka, M., Ishizaki, H., Miyoshi, J., Matsumoto, M., and Seya, T. (2007) *Proc. Natl. Acad. Sci. U.S.A.* **104,** 252–257
10. Mata-Haro, V., Cekic, C., Martin, M., Chilton, P. M., Casella, C. R., and Mitchell, T. C. (2007) *Science* **316,** 1628–1632
11. Imai, Y., Kuba, K., Neely, G. G., Yaghubian-Malhami, R., Perkmann, T., van Loo, G., Ermolaeva, M., Veldhuizen, R., Leung, Y. H., Wang, H., Liu, H., Sun, Y., Pasparakis, M., Kopf, M., Mech, C., Bavari, S., Peiris, J. S., Slutsky, A. S., Akira, S., Hultqvist, M., Holmdahl, R., Nicholls, J., Jiang, C., Binder, C. J., and Penninger, J. M. (2008) *Cell* **133,** 235–249
12. Funami, K., Sasai, M., Ohba, Y., Oshiumi, H., Seya, T., and Matsumoto, M. (2007) *J. Immunol.* **179,** 6867–6872
13. Matsumoto, M., Funami, K., Tanabe, M., Oshiumi, H., Shingai, M., Seto, Y., Yamamoto, A., and Seya, T. (2003) *J. Immunol.* **171,** 3154–3162
14. Kagan, J. C., Su, T., Horng, T., Chow, A., Akira, S., and Medzhitov, R. (2008) *Nat. Immunol.* **9,** 361–368
15. Funami, K., Sasai, M., Oshiumi, H., Seya, T., and Matsumoto, M. (2008) *J. Biol. Chem.* **283,** 18283–18291
16. Sato, S., Sugiyama, M., Yamamoto, M., Watanabe, Y., Kawai, T., Takeda, K., and Akira, S. (2003) *J. Immunol.* **171,** 4304–4310
17. Fitzgerald, K. A., McWhirter, S. M., Faia, K. L., Rowe, D. C., Latz, E., Golenbock, D. T., Coyle, A. J., Liao, S. M., and Maniatis, T. (2003) *Nat. Immunol.* **4,** 491–496
18. Sharma, S., tenOever, B. R., Grandvaux, N., Zhou, G. P., Lin, R., and Hiscott, J. (2003) *Science* **300,** 1148–1151
19. Meylan, E., Burns, K., Hofmann, K., Blancheteau, V., Martinon, F., Kelliher, M., and Tschopp, J. (2004) *Nat. Immunol.* **5,** 503–507
20. Kaiser, W. J., and Offermann, M. K. (2005) *J. Immunol.* **174,** 4942–4952
21. Sasai, M., Oshiumi, H., Matsumoto, M., Inoue, N., Fujita, F., Nakanishi, M., and Seya, T. (2005) *J. Immunol.* **174,** 27–30
22. Häcker, H., Redecke, V., Blagoev, B., Kratchmarova, I., Hsu, L. C., Wang, G. G., Kamps, M. P., Raz, E., Wagner, H., Häcker, G., Mann, M., and Karin, M. (2006) *Nature* **439,** 204–207
23. Oganesyan, G., Saha, S. K., Guo, B., He, J. Q., Shahangian, A., Zarnegar, B., Perry, A., and Cheng, G. (2006) *Nature* **439,** 208–211
24. Horiuchi, M., Sakakibara, H., Kumeta, H., Takahashi, K., Enokizono, A., Ishii, A., Matsumoto, M., Seya, T., and Inagaki, F. (2008) *Biochem. Mol. Biol. Abstr.* **31,** 533
25. Honda, K., and Taniguchi, T. (2006) *Nat. Rev. Immunol.* **6,** 644–658
26. Sasai, M., Tatematsu, M., Oshiumi, H., Funami, K., Matsumoto, M., Hatakeyama, S., and Seya, T. (2010) *Mol. Immunol.* **47,** 1283–1291
27. Salem, M. L., Kadima, A. N., Cole, D. J., and Gillanders, W. E. (2005) *J. Immunother.* **28,** 220–228
28. Seya, T., and Matsumoto, M. (2009) *Cancer Immunol. Immunother.* **58,** 1175–1184
29. Longhi, M. P., Trumpfheller, C., Idoyaga, J., Caskey, M., Matos, I., Kluger, C., Salazar, A. M., Colonna, M., and Steinman, R. M. (2009) *J. Exp. Med.* **206,** 1589–1602
30. Yoneyama, M., and Fujita, T. (2009) *Immunol. Rev.* **227,** 54–65
31. Seth, R. B., Sun, L., Ea, C. K., and Chen, Z. J. (2005) *Cell* **122,** 669–682
32. Matsumoto, M., and Seya, T. (2008) *Adv. Drug Deliv. Rev.* **60,** 805–812
33. Funami, K., Matsumoto, M., Oshiumi, H., Akazawa, T., Yamamoto, A., and Seya, T. (2004) *Int. Immunol.* **16,** 1143–1154
34. Iwamura, T., Yoneyama, M., Yamaguchi, K., Suhara, W., Mori, W., Shiota, K., Okabe, Y., Namiki, H., and Fujita, T. (2001) *Genes Cells* **6,** 375–388

OPEN ACCESS Freely available online

PLoS one

The Peptide Sequence of Diacyl Lipopeptides Determines Dendritic Cell TLR2-Mediated NK Activation

Masahiro Azuma[1☯], Ryoko Sawahata[1☯], Yuusuke Akao[1☯¤a], Takashi Ebihara[1¤b], Sayuri Yamazaki[1], Misako Matsumoto[1], Masahito Hashimoto[2], Koichi Fukase[3], Yukari Fujimoto[3], Tsukasa Seya[1]*

1 Department of Microbiology and Immunology, Graduate School of Medicine, Hokkaido University, Sapporo, Japan, **2** Department of Nanostructure and Advanced Materials, Kagoshima University, Kagoshima, Japan, **3** Department of Chemistry, Graduate School of Science, Osaka University, Toyonaka, Japan

Abstract

Natural killer (NK) cells are lymphocyte effectors that are activated to control certain microbial infections and tumors. Many NK-activating and regulating receptors are involved in regulating NK cell function. In addition, activation of naïve NK cells is fundamentally triggered by cytokines or myeloid dendritic cells (mDC) in various modes. In this study, we synthesized 16 S-[2,3-bis(palmitoyl)propyl]cysteine (Pam2Cys) lipopeptides with sequences designed from lipoproteins of *Staphylococcus aureus*, and assessed their functional properties using mouse (C57BL/6) bone marrow-derived DC (BMDC) and NK cells. NK cell activation was evaluated by three criteria: IFN-γ production, up-regulation of NK activation markers and cytokines, and NK target (B16D8 cell) cytotoxicity. The diacylated lipopeptides acted as TLR2 ligands, inducing up-regulation of CD25/CD69/CD86, IL-6, and IL-12p40, which represent maturation of BMDC. Strikingly, the Pam2Cys lipopeptides induced mouse NK cell activation based on these criteria. Cell-cell contact by Pam2Cys peptide-stimulated BMDC and NK cells rather than soluble mediators released by stimulated BMDC induced activation of NK cells. For most lipopeptides, the BMDC TLR2/MyD88 pathway was responsible for driving NK activation, while some slightly induced direct activation of NK cells via the TLR2/MyD88 pathway in NK cells. The potential for NK activation was critically regulated by the peptide primary sequence. Hydrophobic or proline-containing sequences proximal to the N-terminal lipid moiety interfered with the ability of lipopeptides to induce BMDC-mediated NK activation. This mode of NK activation is distinctly different from that induced by polyI:C, which is closely associated with type I IFN-inducing pathways of BMDC. These results imply that the MyD88 pathway of BMDC governs an alternative NK-activating pathway in which the peptide sequence of TLR2-agonistic lipopeptides critically affects the potential for NK activation.

Citation: Azuma M, Sawahata R, Akao Y, Ebihara T, Yamazaki S, et al. (2010) The Peptide Sequence of Diacyl Lipopeptides Determines Dendritic Cell TLR2-Mediated NK Activation. PLoS ONE 5(9): e12550. doi:10.1371/journal.pone.0012550

Editor: Jacques Zimmer, Centre de Recherche Public de la Santé, Luxembourg

Received June 10, 2010; **Accepted** July 30, 2010; **Published** September 2, 2010

Funding: This work was supported in part by Grants-in-Aid from the Ministry of Education, Science, and Culture (Specified Project for Advanced Research) and the Ministry of Health, Labor, and Welfare of Japan, and by the Yakult and Waxmann Foundations. Financial support by the Sapporo Biocluster "Bio-S" the Knowledge Cluster Initiative of the MEXT, is gratefully acknowledged. The funders had no role in study design, data collection and analysis, decision to publish, or preparation of the manuscript.

Competing Interests: The authors have declared that no competing interests exist.

* E-mail: seya-tu@pop.med.hokudai.ac.jp

☯ These authors contributed equally to this work.

¤a Current address: Yakult Central Institute for Microbiological Research, Kunitachi, Tokyo, Japan
¤b Current address: Howard Hughes Medical Institute, Washington University School of Medicine, St. Louis, Missouri, United States of America

Introduction

Natural killer (NK) cells function in early defense against various pathogens. Microbial pattern molecules activate NK cells by stimulating pattern-recognition receptors (PRRs) in NK cells or myeloid dendritic cells (mDC) [1]. mDC-mediated NK activation occurs secondary to mDC maturation, and is competent to induce NK-activating cytokines or mDC membrane molecules to facilitate reciprocal activation of mDC and NK cells [1,2]. Toll-like receptors (TLRs) and cytoplasmic pattern sensors are PRRs that may be associated with mDC-mediated NK activation [1,3]. In mDC, TLR3 and cytoplasmic sensors, RIG-I/MDA5 usually participate in driving NK activation in response to double-stranded (ds)RNA [4–6].

Staphylococcus aureus, a versatile Gram-positive pathogen, is reported to activate NK cells during infection [7]. *S. aureus* cell wall components including peptidoglycan, lipoproteins, and alanylated lipoteichoic acid, are inflammation inducers, and provoke the activation of host immune cells [8]. *S. aureus* cell wall pattern molecules are mainly recognized by cell-surface TLR2 and cytoplasmic nucleotide-binding oligomerization domain 2 (Nod2) in host cells, which signal the presence of bacterial infection. Mice lacking TLR2 or the adaptor protein MyD88 are highly susceptible to *S. aureus* infection [9]. The molecular basis by which *S. aureus* activates host immunity has been investigated, and lipoprotein, rather than lipoteichoic acid, is the main trigger of immune stimulation [10] that preferentially activates TLR2 in mouse cells. TLR2/MyD88 determines the pathway for activation of macrophages in mice [11]. Lipoprotein also activates TLR2 in human cells [12,13].

The functional properties of *S. aureus* lipopeptides have been investigated in gene-disrupted mice [9,14,15]. TLR2, in concert with TLR1 or TLR6, is involved in their recognition [16,17]. Two adaptor proteins, TIRAP and MyD88, deliver TLR2 signals that

activate NF-κB [18,19], which functions in cytokine induction. These studies were mainly performed in mouse macrophages, and results were essentially consistent with other biochemical studies using macrophages [20,21]. Nonetheless, more complicated regulation may occur in other immune-related cells, including mDCs. Recent studies suggested that in mDCs, TLR2 and MyD88 are involved in NK activation that is provoked by bacterial pattern molecules [22,23]. Our previous results also inferred that bacterial lipoproteins act as TLR2 agonists in mDC-driven NK activation [24].

In mDCs, a subset of the antigen-presenting cells, the two major arms of the innate immune signaling pathway, the MyD88 and TICAM-1 (TRIF) pathways, function in the TLR signaling [18,19]. In addition, cytokines including IL-12, IL-15 and IFN-α/β, as well as DC-NK contact are involved in NK cell activation [25,26]. TLR3 is a sensor of dsRNA and induces mDC maturation via TICAM-1 [4,25]. A characteristic feature of TLR3-TICAM-1-mediated mDC maturation is liberation of IL-12, and, independent of IL-12, drives NK cell activation [4]. On the other hand, what factors participate in TLR2-MyD88-mediated mDC maturation to drive NK activation remains largely unknown.

We identified lipopeptides from Triton X-114-solubilized *S. aureus* cells [27,28]. Since *S. aureus* lacks lipoprotein N-acyltransferase, these lipoproteins are predicted to be S-[2,3-bis(palmitoyl)-propyl]cysteines (Pam2Cys) [29]. Their diacylated structure was confirmed by MS/MS spectrometry [28]. We annotated these lipoproteins by function, which largely depends on their protein sequence [30]. Based on these results, we chemically synthesized 16 Pam2Cys lipopeptides of 6–18 amino acids (a.a.) [30]. They possessed TLR2 agonistic activity, but varied in their functional potential to activate NF-κB and liberate TNF-α from human PBMC [30], yet their NK activation potential has not been determined.

This study shows that naïve NK cells are usually in a resting state, and bacterial lipoproteins trigger mDC-mediated NK activation in response to TLR2-derived cellular events. We found that mDC maturation and NK activation are strongly modulated by the amino acid (a. a.) sequence of TLR2 agonistic lipopeptides.

Results

Cytokines liberated from BMDC in response to Pam2 peptides

We synthesized 16 Pam2Cys-containing lipopeptides using *S. aureus* lipoproteins as a reference [30], and designated them Pam2Cys1-Pam2Cys16 (Table 1). Included as positive controls were the diacyl lipopeptides Pam2CSK4 [31], designated as Pam2CSK19 in this study, and its derivatives Pam2CSK (Pam2Cys17), and Pam2CSK2 (Pam2Cys18). Pam2Cys17 was used as a negative control, since this diacyl lipopeptide has virtually no cytokine-inducing activity (Fig. 1). ELAM-luciferase reporter assays were used to assess the NF-κB activation potential of these lipopeptides at 10–500 nM, and a representative result for 100 nM is in Figure 1A. Pam2Cys18 and 19 showed high reporter activity, but Pam2Cys17 did not (Fig. 1A). A series longer than 3 a. a were essential for TLR2 stimulation. The level of TNF-α liberated from mouse BMDC was largely comparable with that induced by human PBMC (Table 1). Pam2Cys4, Pam2Cys13, Pam2Cys15 and Pam2Cys16 exhibited relatively low NF-kB activation and TNF-α production (Table 1, Fig. 1A).

IL-6 and IL-12p40 levels were determined by ELISA using the supernatant of the media from bone marrow-derived DC (BMDC) culture with the lipopeptides for 24 h. The cytokines were detected at high levels in the cultures with lipopeptides, with the exception of Pam2Cys17, Pam2Cys13, and Pam2Cys16 (Fig. 1B,C). The cytokine contents of wells with BMDCs stimulated with Pam2Cys13 and Pam2Cys16 were as low as the control Pam2Cys17.

Table 1. Pam2 lipopeptides used for this study.

No.	Lipid	Amino acid sequence	TNF-α*
Pam2Cys1	Pam2	CANTRHSESDK	++
Pam2Cys2	Pam2	CGTGGKQSSDK	++
Pam2Cys3	Pam2	CGNGNKSGSDD	++
Pam2Cys4	Pam2	CSNIEIFNAKG	+/−
Pam2Cys5	Pam2	CTTDKKEIKAY	+++
Pam2Cys6	Pam2	CSFGGNHKLSS	++
Pam2Cys7	Pam2	CGSQNLAPLEE	+++
Pam2Cys8	Pam2	CGQDSDQQKDG	+++
Pam2Cys9	Pam2	CGNDDGKDKDG	+++
Pam2Cys10	Pam2	CGNNSSKDKEA	+++
Pam2Cys11	Pam2	CSLPGLGSKST	+++
Pam2Cys12	Pam2	CSTSEVIGEKI	++
Pam2Cys13	Pam2	CPFNCVGCYNK	+/−
Pam2Cys14	Pam2	CGSQNLAPLEEK	+/−
Pam2Cys15	Pam2	CLILIIASETL	+/−
Pam2Cys16	Pam2	CLILIIASETLFSFSHLTDVK	+/−
Pam2Cys17	Pam2	CSK	n.d.
Pam2Cys18	Pam2	CSKK	n.d.
Pam2Cys19	Pam2	CSKKKK	++

*100 pg/ml of Pam2 peptides were used for stimulation of PBMC.
TNF-α levels: +/−; <200, ++; 2,000–4,000, +++; 4,000–7,000 pg/ml.
n.d., not determined.
doi:10.1371/journal.pone.0012550.t001

The degree of CD86 upregulation by the 16 *S. aureus* lipopeptides was examined, and similar DC maturation profiles were obtained by flow cytometer for all Pam2Cys tested (Fig. 1D), suggesting BMDC maturation, as determined by CD86 up-regulation, was independent of NF-kB activation or cytokine liberation by these lipopeptides.

NK activation by Pam2Cys peptides

Previous reports suggested that TLR2 agonists can induce NK activation [22–24]. To investigate whether the *S. aureus* lipoproteins had NK cell-activating activity, we added the Pam2Cys peptides at 100 nM to BMDC/NK cultures as described previously [4]. Three markers for NK activation [26] were assessed: IFN-γ production, up-regulation of NK surface markers, and target B16D8 cell cytotoxicity by NK cells (Fig. 2). IFN-γ was generated in the supernatants (sup) in response to the lipopeptides (Fig. 2A). However, Pam2Cys13, Pam2Cys15, and Pam2Cys16 showed significantly low potential for IFN-γ induction as comparable to Pam2Cys17. Cytotoxic activity was evaluated using B16D8 cells as a target [4]. Again, Pam2Cys13, 15 and 16 did not induce effective killing (Fig. 2B). The other *S. aureus* lipopeptides had sufficient killing activity: two simultaneously generated examples are shown in Figure 2B.

The NK cell activation markers CD25 and CD69 were analyzed by flow cytometry after co-culturing NK cells with BMDC and Pam2Cys stimulants (Fig. 2C). Up-regulation of

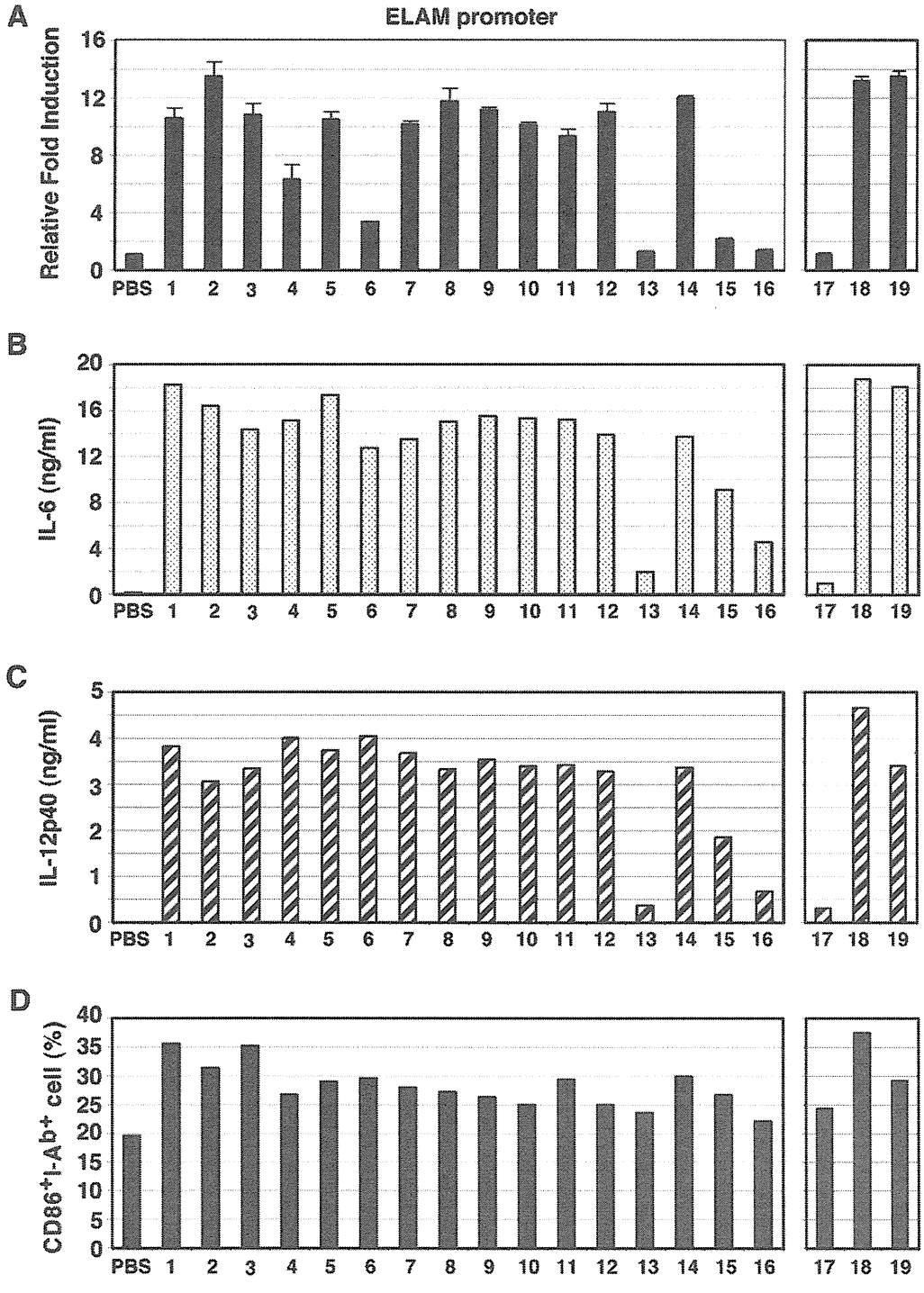

Figure 1. Synthetic Pam2Cys lipopeptides activate TLR2 and induce cytokine production in BMDC. (A) HEK293 cells were transfected with plasmids encoding TLR2 and ELAM-luciferase reporter. After 24 h, the cells were treated with Pam2Cys peptides (100 nM) for 6 h and then luciferase activities of the cell lysates were measured. (B, C) BMDC were treated with Pam2Cys peptides for 24 h and IL-6 and IL-12p40 concentrations in the culture supernatants were measured by ELISA. (D) CD86 and MHC class II (I-Ab) expression of the BMDC were determined by flow cytometry. Data represents the mean ± SD of triplicate measurements. The data shown are representative of at least three independent experiments. The numbers represent the Pam2Cys's numbers.
doi:10.1371/journal.pone.0012550.g001

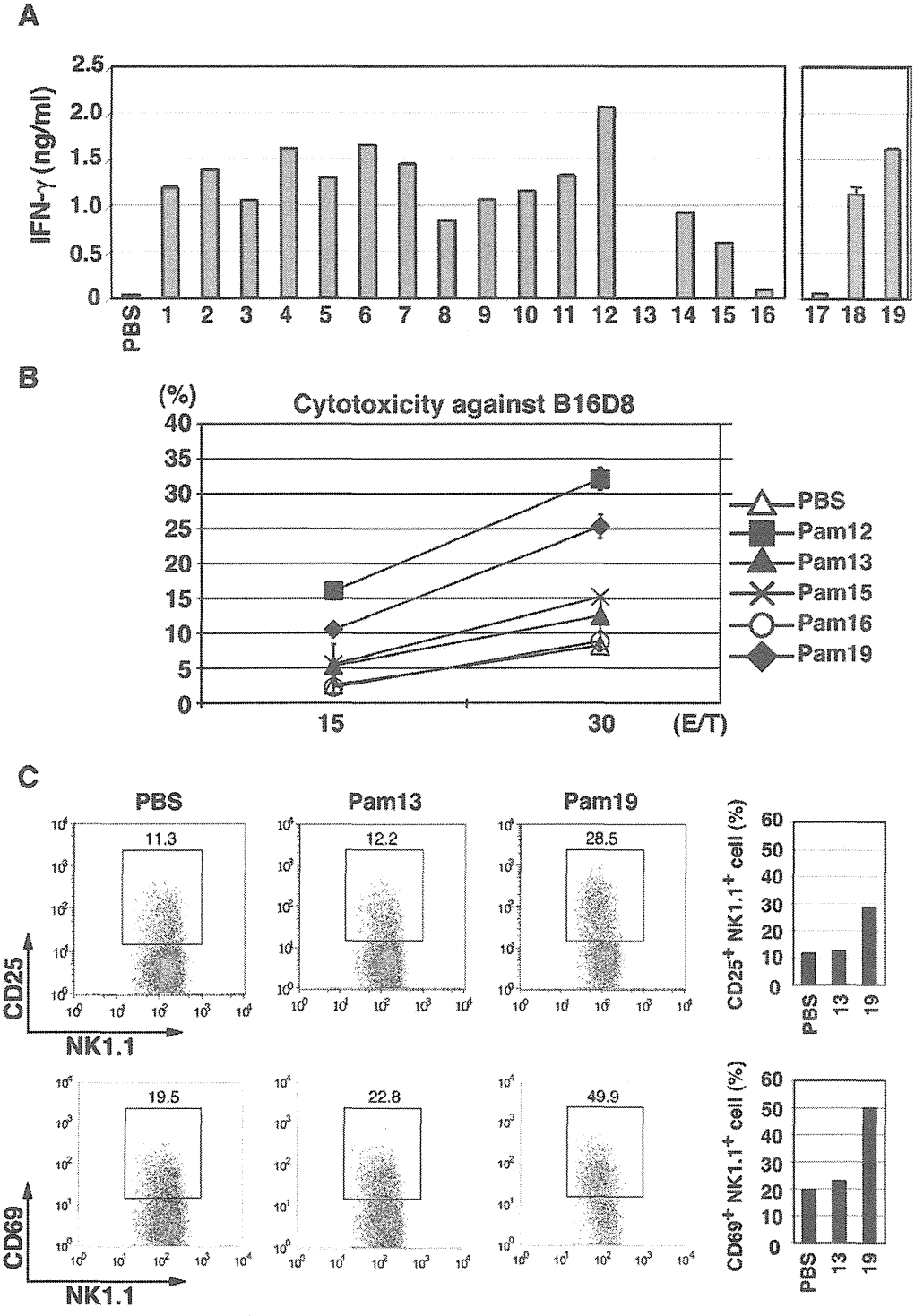

Figure 2. Pam2Cys peptides activate NK cells via BMDC. (A) Wild-type BMDC and wild-type NK cells were co-cultured at 1:2 ratio in the presence of Pam2Cys peptides as the numbers indicated (100 nM). After 24 h, IFN-γ concentrations in the supernatants were measured by ELISA. (B) NK cell cytotoxicity against B16D8 cells was measured by ^{51}Cr release assay at indicated E:T ratios as described in the Methods section. (C) Populations of CD25+ and CD69+ NK cells were measured by flow cytometry after stimulation of NK cells with BMDC treated with indicated Pam2Cys peptides. BMDC were stimulated with control PBS, 100 nM of Pam2Cys13 or Pam2Cys19 for 4 h. Then, BMDC were incubated with NK cells. After 24 h, cells were analyzed by flow cytometer using the markers for separation. %Positive cells are shown to the right.
doi:10.1371/journal.pone.0012550.g002

surface CD25 and CD69 was observed in NK cells incubated with BMDC and Pam2Cys18 or 19, while the levels of their up-regulation by Pam2Cys13, 15 or 16 were near those of the negative control Pam2Cys17, for stimulating NK cells co-cultured with BMDC. In contrast, no increase was observed for CD56, NKp46 and DNAM-1 (data not shown).

Participation of TLR2/MyD88 in Pam2Cys-mediated BMDC and NK activation

Activated NK cells are a major source of IFN-γ, which causes a variety of responses in the immune system. To examine whether direct stimulation of NK cells with Pam2Cys18 or Pam2Cys19 induced secretion of IFN-γ, we measured the frequency of IFN-γ-secreting NK cells, at 24 h after incubation. By intracellular staining, IFN-γ-secreting NK cells were increased after direct Pam2Cys18 or 19 stimulation (data not shown). As shown in Figure 3A and B, TLR2 ligands except Pam2Cys12, 18 and 19 barely increased the levels of IFN-γ of NK cells by co-culture with Pam2Cys-stimulated TLR2−/− or MyD88−/− BMDC. On the other hand, NK cells induce moderate levels of IFN-γ in response to BMDC stimulated with Pam2Cys12, 18 or 19 (open bars in Figure 3A), although no structural similarity was detected between Pam2Cys12 and Pam2Cys18 or 19.

We next examined whether lipopeptide-mediated cytokine secretion and NK activation were dependent on BMDC TLR2 and MyD88. IL-6 and IL-12p40 secretion were completely abrogated in TLR2−/− BMDC (data not shown). However, low amounts of IFN-γ were detected in co-cultures of TLR2−/− or MyD88−/− BMDC and wild-type (WT) NK cells in the presence of Pam2Cys12, 18, or 19 (Fig. 3B,D), and lesser extent of IFN-γ was still detected in co-cultures of WT BMDC and TLR2−/− NK cells in the presence of Pam2Cys12 or Pam2Cys19 (Fig. 3C). These results were reproduced with MyD88−/− BMDC (not shown). Notable results are shown in Fig. 3D where WT or TLR2−/− BMDC were stimulated with indicated Pam2Cys and incubated with WT or TLR2−/− NK cells. Moderate IFN-γ was detected in the media containing TLR2−/− BMDC, WT NK and Pam2Cys12 or 19 (Fig. 3D), the IFN-γ levels being comparable to those of WT NK cells alone stimulated with Pam2Cys12 or 19 (Fig. S1). TLR2−/− NK cells still produced very low levels of IFN-γ when the TLR2−/− NK cells were co-cultured with WT BMDC (Fig. 3D). However, No IFN-γ was detected in the media containing TLR2−/− NK and Pam2Cys12 or 19. Thus, all Pam2Cys peptides including Pam2Cys12, 18 and 19 act on BMDC to drive NK activation. Notably, WT NK cells alone produce minute IFN-γ in response to Pam2Cys12 or 19 (Fig. S1), which means that Pam2Cys12 and Pam2Cys19 additionally induce direct NK activation. The Pam2Cys receptors for this NK activation is through the NK cell TLR2 followed by the MyD88 pathway. However, minute activation by Pam2Cys12 or 18/19 appears to be left in TLR2−/− NK cells stimulated with Pam2Cys12/19-treated BMDC, which should be attributed not to TLR2 but to other unknown mechanisms.

Combinatorial recognition of Pam2Cys lipopeptide by TLR2 and TLR6

TLR2 recognizes diacyl lipopeptides in combination with TLR6 [14,31] while TLR2 recognizes triacyl lipopeptide with TLR1 [15,32]. We found TLR2/6 cooperation in the recognition of *S. aureus* lipopeptides using HEK293 cells that express TLR2/6. Data on the use of TLR2/6 by Pam2Cys12, Pam2Cys13, Pam2Cys15, Pam2Cys16, and Pam2Cys19 is shown in Figure 4. Single receptors of TLR1, TLR6, and TLR10 showed little activation of NF-κB by reporter assay, and only TLR2 exhibited <60-fold ELAM promoter activation (data not shown). Pam2Cys12 and Pam2Cys17 more efficiently activated the ELAM promoter (>300 fold over the control) with TLR2 and 6, than with TLR2 alone (Fig. 4A). TLR1 or TLR10 in combination with TLR2 did not amplify the signal (Fig. 4B). Pam2Cys13 only weakly enhanced the TLR2 potential with additional TLR6 expression in HEK cells (Fig. 4A), and only a slight increase was observed with Pam2Cys15 and Pam2Cys16 with simultaneous expression of TLR2 and TLR6 (Fig. 4A). Hence, TLR6 helped TLR2 to amplify the TLR2 signal from most Pam2Cys lipopeptides, but not with Pam2Cys13 or Pam2Cys15/16.

Critical a.a. in Pam2Cys lipopeptides for BMDC-mediated NK activation

Recent studies revealed an extensive cross-talk between NK cells and mDCs [2,6]. We analyzed the structural background that supports NK activation using our synthetic diacyl lipopeptides. All NK-activating lipopeptides tested had Cys-Ser/Thr or Cys-Gly/Ala in their N-terminus (Table 1). However, the two lipopeptides with the lowest ability to activate NK cells had differences, with Cys-Pro in the N-terminus of Pam2Cys13, and Cys-Leu-Ile in Pam2Cys15/16. When the second Pro in Pam2Cys13 was replaced with Ser, and the Leu-Ile sequence of Pam2Cys16 was replaced with Ser-Asn, the newly synthesized peptides, Pam2-Cys13(P-S) and Pam2Cys16(LI-SN), recovered their ELAM reporter activity (Fig. 5A).

We next tested whether BMDC mature to activate NK cells through BMDC's TLR2 activation by these modified Pam2Cys. Pam2Cys13(P-S) and Pam2Cys15(LI-SN) recovered NK-activating properties by the amino acid conversions judged by IFN-γ production (Fig. 5B) and cytotoxicity against B16D8 cells (Fig. 5C). Since Pam2Cys13(P-S) acts only on BMDC (not shown), this Pam2Cys activity is attributable to recovered BMDC maturation. Hence, Pam2Cys13(P-S) and Pam2Cys16(LI-SN) are NK activators via mDC TLR2. Hence, we conclude that the peptide sequence near the N-terminus is important for NK activation by diacyl lipopeptide.

Production of both IL-6 and IL-12p40 was dependent on BMDC TLR2 (Fig. 6A). Pam2Cys13 and Pam2Cys16 induced these cytokines at very low levels. When Pam2Cys13(P-S) or Pam2Cys16(LI-SN) replaced Pam2Cys13 or Pam2Cys16 in the same assay system, the cytokine levels recovered to levels similar to those of the other lipopeptides (Fig. 6B). These activities were almost completely abrogated in TLR2−/− BMDCs. Thus, the a.a. replacements allows BMDC to generate the TLR2 signal, irrespective of their artificial modifications.

BMDC-NK contact is indispensable for BMDC TLR2-mediated NK activation

Pam2Cys13(P-S) matured BMDC to activate NK cells without direct action on NK cells (Fig. 7A). First, we collected the sup of BMDC stimulated with Pam2Cys13 or Pam2Cys13(P-S). Surprisingly, Both of the sup failed to confer NK activating function on the mixture of naïve BMDC and NK cells (data not shown). The capacity of BMDC sup to induce IFN-γ-secretion by NK cells was further evaluated using a transwell system (Fig. 7A,B). No significant increase in IFN-γ-secreting NK cells was observed when lipopeptide-activated BMDCs and NK cells were separated by transwell (Fig. 7A,B). Frequency of IFN-γ-producing NK cells was high in co-culture with Pam2Cys13(P-S)-stimulated BMDC and NK cells (Fig. 7B upper panel) while the IFN-γ-producing NK

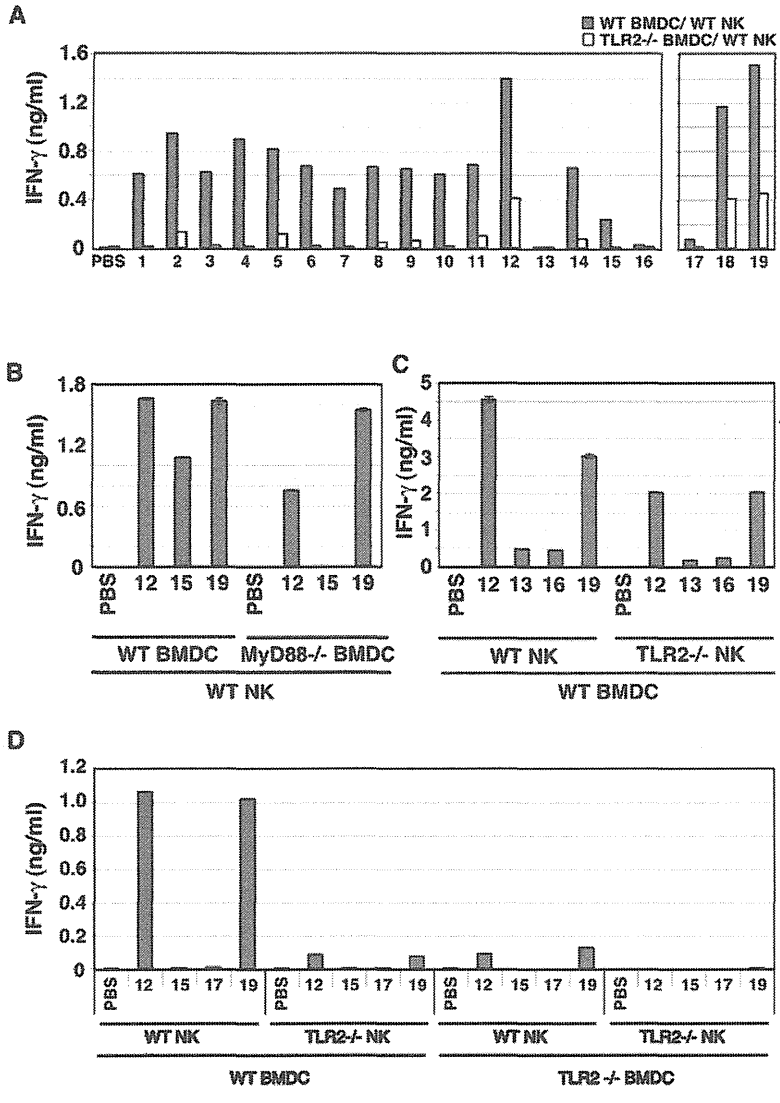

Figure 3. TLR2 on BMDC mainly participate in Pam2Cys-mediated NK activation. (A) BMDC TLR2-independent NK activation by Pam2Cys12, 18 and 19. BMDC from wild-type (closed bars) or TLR2−/− (open bars) mice were stimulated with control PBS or 100 nM of indicated Pam2Cys peptides for 4 h. Cells were then co-cultured with wild-type NK cells at 1:2 ratio for 24 h. Then, the supernatants were collected and IFN-γ was measured by ELISA. (B) Pam2Cys12 and 19 induce NK activation in culture with MyD88−/− BMDC. NK cells were co-cultured with wild-type or MyD88−/− BMDC in the presence of the indicated Pam2Cys peptides (represented by the numbers) as in Fig. 2. 24 h after incubation, culture media were collected to determine cytokines by ELISA. (C) Pam2Cys12 and 19 induce TLR2−/− NK activation in culture with wild-type BMDC. Wild-type BMDC and NK cells with either wild-type or TLR2−/− phenotype were incubated at 1:2 ratio with the indicated Pam2Cys peptides (represented by the numbers) as in Fig. 2. 24 h after incubation, culture media were collected to determine cytokines by ELISA. One representative of the three similar experiments is shown. (D) TLR2 NK cells mainly participates in TLR2 BMDC-independent NK activation by Pam2Cys12 and 19. Wild-type and TLR2−/− BMDC were stimulated with indicated Pam2Cys peptides for 4 h. These BMDC were then mixed with NK cells as shown in the panel. Four groups consisting of either of wild-type NK or TLR2−/− NK and either of wild-type BMDC or TLR2−/− BMDC (see the bottom of the panel) were incubated with the indicated Pam2Cys peptides (50 nM) for 24 h. NK cells alone with Pam2Cys12 or 19 liberated minure IFN-γ as in the panel with WT NK + TLR2−/− BMDC (see Fig. S1). IFN-γ concentrations in the culture supernatants were determined by ELISA. The data shown are representative of at least three independent experiments.
doi:10.1371/journal.pone.0012550.g003

cells were diminished in the transwell (Fig. 7B lower panel). In either case, IL-15 and IFN-α/β were barely increased in Pam2Cys-stimulated BMDCs by RT-PCR (data not shown). Thus, soluble factors barely participate in BMDC-mediated NK activation. BMDC-NK contact is essential for TLR2-mediated NK activation.

Discussion

Here, we demonstrated that the a. a. sequence of *S. aureus* Pam2Cys peptides critically affects the agonistic function for TLR2 and the mode of NK activation. This NK activation is largely dependent on TLR2/MyD88 in BMDC in the mouse

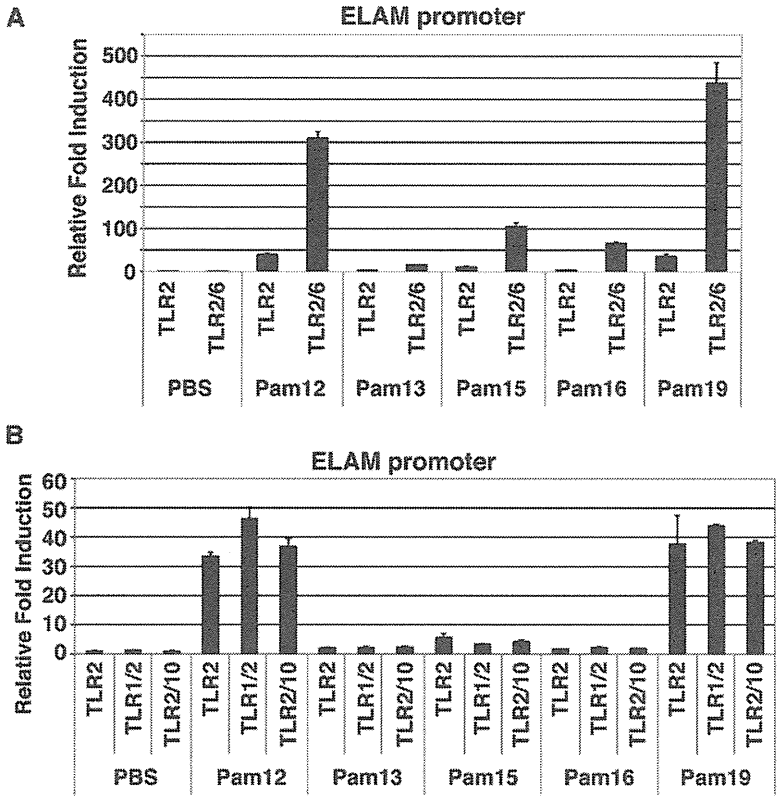

Figure 4. TLR6 promotes TLR2 signaling in Pam2Cys peptides recognition. (A, B) HEK293 cells were transfected with plasmids encoding TLR2, TLR6, TLR1 or TLR10 and the ELAM-luciferase reporter. After 24 h, the cells were treated with indicated Pam2Cys peptides (100 nM) for 6 h and then luciferase activities were measured. The data shown are representative of at least three independent experiments.
doi:10.1371/journal.pone.0012550.g004

system. In addition, Pam2Cys12 and Pam2Cys18/19 have a weak ability to directly activate NK cells without participation of BMDC. In contrast, we determined Pam2Cys13, Pam2Cys15, and Pam2Cys16 to be dysfunctional, since these lipopeptides failed to activate TLR2/6 reporter signaling or induce cytokines in BMDC (Fig. 1,4). Although the first Cys is conserved in all the lipopeptides tested, the following sequences varied, even though all showed BMDC maturation activity. Notably, the second a. a. residue was Ser/Thr or Gly/Ala in the functional lipopeptides, followed by undefined sequences. A length of more than three a.a. was indispensable for BMDC-mediated NK activation (Fig. 1, Pam2Cys17 vs. 18). The failure of Pam2Cys13, Pam2Cys15, and Pam2Cys16 to activate NK cells suggests the importance of the second and/or third residue for stimulating BMDC or directing NK activation. Pam2Cys13 harbors Pro in the second residue, which breaks hydrogen bond interactions. Likewise, Pam2Cys15 and Pam2Cys16 commonly possess Leu and ILe in the second and third residues, which also destabilize hydrogen bond interactions. Thus, these a. a. residues critically influence the effectual interaction between the Pam2Cys peptides and the TLR2 complex on either BMDC or NK cells.

TLR2 initiates immune response by recognizing diacylated lipoproteins in combination with TLR6. We surmise that this receptor complex recognizes the a. a. properties in the peptide sequence that activate mDC/NK cells. Crystal structure analysis indicates that hydrogen bonds between glycerol and the peptide backbone of the ligand and the leucine-rich repeat (LRR)11 loops of TLRs are critical for TLR heterodimerization [31,32]. These hydrogen bonds bridge TLR2 and TLR6 with the ligand, and fix the conformation of the hydrophobic residues around the dimerization interface [31]. The side chains of the first two a. a. of Pam2Cys have substantial interactions with the TLRs. The N-terminal Cys binds to the sulfur site formed by the hydrophobic F325, L328, F349, L350, and P352 residues of TLR2, and the L318 residue of TLR6 [31]. The hydroxyl side chains of the second Ser/Thr form a medium-range hydrogen bond with the F325 backbone of TLR2. As seen in the TLR2/TLR6/Pam2CSK4 structure, the side chains beyond the third lysine residue have highly flexible structures and form only weak ionic or hydrogen bond interactions with the TLRs [31]. Hence, our results with a. a. substitutions fit the proposed TLR2-Pam2CSK4 interacting model.

In a previous report, lysines in the triacyl peptide were seen to form hydrogen bonds with TLRs when Pam3CSK4 interacts with TLR2/TLR1 heterodimer [32]. The ε-amino residues in the side chains appear to participate in lipopeptide recognition by TLRs [31,32]. In our results, the small side chains of Asn or Gly had no blocking effects on the peptide-TLR2 interaction (data not shown). Thus, a hydrophilic or small a. a. in the chain barely altered the lipopeptide function exerted through TLR2. The *S. aureus* lipopeptides, with the exception of Pam2Cys13, Pam2Cys15, and Pam2Cys16 are compatible with this principle. We actually demonstrated here that the peptide sequences have a significant effect on the immunological activity of the lipopeptides. The recognition system for bacterial lipoproteins has developed to